DOI: 10.1002/anie.200905335

Biofuels

Biofuel Combustion Chemistry: From Ethanol to Biodiesel

Katharina Kohse-Höinghaus, Patrick Oßwald, Terrill A. Cool, Tina Kasper, Nils Hansen, Fei Qi, Charles K. Westbrook, and Phillip R. Westmoreland*

Keywords:
biofuel · biomass · combustion · mass spectrometry · reactive intermediates

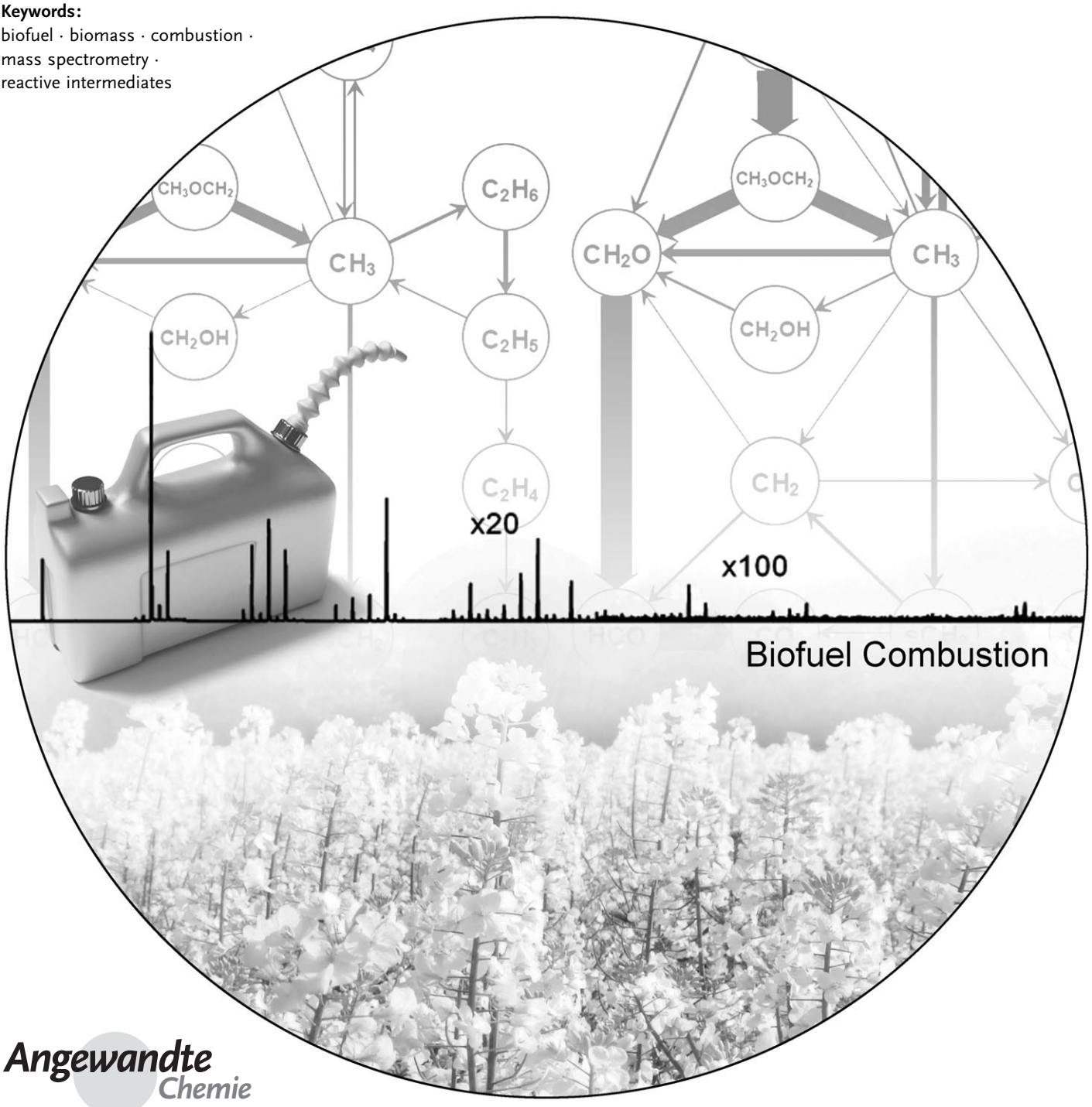

Biofuels, such as bio-ethanol, bio-butanol, and biodiesel, are of increasing interest as alternatives to petroleum-based transportation fuels because they offer the long-term promise of fuel-source regenerability and reduced climatic impact. Current discussions emphasize the processes to make such alternative fuels and fuel additives, the compatibility of these substances with current fuel-delivery infrastructure and engine performance, and the competition between biofuel and food production. However, the combustion chemistry of the compounds that constitute typical biofuels, including alcohols, ethers, and esters, has not received similar public attention. Herein we highlight some characteristic aspects of the chemical pathways in the combustion of prototypical representatives of potential biofuels. The discussion focuses on the decomposition and oxidation mechanisms and the formation of undesired, harmful, or toxic emissions, with an emphasis on transportation fuels. New insights into the vastly diverse and complex chemical reaction networks of biofuel combustion are enabled by recent experimental investigations and complementary combustion modeling. Understanding key elements of this chemistry is an important step towards the intelligent selection of next-generation alternative fuels.

From the Contents

1. Introduction

In this Review, a summary of recent investigations of the combustion chemistry of prototypical biofuel components is presented. Biofuels may be used for different purposes in energy conversion, including road transport, aviation, and electricity generation. In the public discussion, the term biofuel is associated with only a few selected compounds, especially ethanol and the very large methyl esters in biodiesel. Other biofuels, such as *n*-butanol, are rarely discussed. These typical biofuel representatives are oxygenated fuels, containing oxygen as an additional element in their molecular constitution. This feature distinguishes them from the hydrocarbons in conventional petroleum-based fuels, the combustion chemistry of which has long been studied. The presence of the oxygen atom in the oxygenated fuel molecules alters the electronic structure, and almost all the C–H bond strengths for the oxygenated fuels are different from their values for structurally related, more familiar hydrocarbon fuels. To understand the associated combustion reactions and to identify recurring reaction patterns, it is important to study prototypical variants of potential biofuels. In this regard, examining the fuel decomposition and oxidation reactions of smaller esters is a valuable step towards understanding the reaction pathways of the large ester molecules found in true-biodiesel, and the combustion mechanisms of ethanol and propanol will be building blocks in a combustion mechanism for larger alcohols. Biomass may contain further chemical elements beyond carbon, hydrogen, and oxygen, and in consequence, studies of the related combustion chemistry must take the chemical variability of such biofuel sources into account.

New insights into the complex reaction pathways associated with the combustion of biofuels and related chemical compounds rely on a multitude of experimental and numerical approaches. It is outside of the scope of this Review to describe all the respective instruments and strategies. Much of the work highlighted herein focuses on the analysis of the species composition of laminar premixed flames by molecular-beam mass spectrometry, and cases in which the experimental results have been complemented with computer simulations, using appropriate combustion models. Some relevant details for this approach are described in Section 3. Combustion chemistry aspects for prototypical oxygenated fuels are presented in Section 4, and arranged in sequence of increasing chemical complexity. As a perspective, some recent examples for the combustion of nitrogenated fuels are then

[*] Prof. K. Kohse-Höinghaus, Dr. P. Oßwald
Department of Chemistry, Bielefeld University
Universitätsstrasse 25, 33615 Bielefeld (Germany)
Fax: (+49) 521-106-6027
E-mail: kkh@pc1.uni-bielefeld.de
Prof. T. A. Cool
School of Applied and Engineering Physics, Cornell University
Ithaca, NY 14853 (USA)
Dr. T. Kasper, Dr. N. Hansen
Combustion Research Facility, Sandia National Laboratories
Livermore, CA 94551 (USA)
Prof. F. Qi
National Synchrotron Radiation Laboratory, University of Science and Technology of China
Hefei, Anhui 230029 (China)
Dr. C. K. Westbrook
Lawrence Livermore National Laboratory
P.O. Box 808, 7000 East Avenue, Livermore, CA 94550 (USA)
Prof. P. R. Westmoreland
Department of Chemical and Biomolecular Engineering, North Carolina State University
Engineering Building I, Box 7905, Raleigh, NC 27695 (USA)

given in Section 5. The discussion of the combustion chemistry of biofuels would be considered incomplete, however, without some context of more general relevance, provided in Section 2, regarding selected aspects of the climatic impact and the production of biofuels.

2. Aspects in the Discussion of Biofuels

2.1. Carbon Dioxide Balance

Recent public and scientific discussions on the potential substitution of conventional petroleum-based transportation fuels by biogenic matter concentrate on climatic, geopolitical, and socio-economic aspects. It is commonly suggested that carbon dioxide emissions from combustion of fossil fuels can be offset by the use of fuels from biomass. Contrary arguments include a potentially unsatisfactory energy balance of the well-to-wheel biofuel production process and the competition of biofuel crops with food plants. Further considerations concern the transformation of pristine ecosystems and loss of biodiversity associated with biofuel plant growth. Also, ancillary processes, such as fertilization or clearing agricultural areas by biomass burning, may contribute to the release of undesired emissions. The magnitude of potential carbon savings from current biomass-to-biofuels processes is being discussed.[1] It is assumed that the carbon debt created from land clearing for biofuel crop production can eventually be paid back by CO_2 saved from biofuel versus fossil-fuel combustion. Large differences may arise, however, depending on the specific strategy. For example, production of biodiesel from palms grown from rainforest areas in Indonesia or Malaysia will release more than 400-times the CO_2 saved, according to model calculations, compared with ethanol produced from prairie biomass on abandoned cropland in the USA, which would generate an approximately zero carbon debt.[1]

2.2. Aerosol and Nitrogen Oxide Emissions

The clearing of land for agricultural use by biomass burning, which often precedes cultivation of biofuel crops, is an important factor in the generation of carbonaceous aerosols. It has a significant climatic impact beyond CO_2 release.[2] From aerosols sampled in India and the Maldives, the contribution to total organic carbon, soot carbon, and elemental carbon from biomass burning (although not only related to biofuel crop cultivation) was estimated from radiocarbon measurements to be 64–76%, 63–78%, and 41–60%, respectively. About two-thirds of the associated climate forcing in the South Asian winter, which may have an impact on monsoon patterns and melting of Himalayan glaciers, is thus attributed to biomass-combustion-generated carbonaceous aerosols.

Nitrogen is a chemical constituent in biological matter, and it is taken up by biofuel crops from fertilization. Nitrogen conversion in combustion is an important subject of research. Biomass burning contributes significantly to NO_x emissions[3] with an inventory, estimated for the year 2000 from satellite-based observations, of 5–5.9 Tg N/year, compared to 2.5–4.5 Tg N/year released from N-fertilized soils and 24–26 Tg N/year from fuel (fossil and biofuel) combustion. The nitrogen content in biofuels varies, and the yield of N_2O from biofuels may be 3–5 times larger than previously assumed.[4] This situation is especially alarming because the global warming potential of N_2O is almost 300-times higher than for CO_2. Rapeseed biofuel, which represents more than 80% of worldwide biodiesel, seems an unsatisfactory choice based on the analysis in Ref. [4] because high amounts of nitrogen fertilizers are typically used for its production; the nitrogen content in rapeseed is reported with 39 g N kg^{-1} dry matter to be much larger than in maize and sugar cane (15 and 7.3 g N kg^{-1}, respectively), which are both used for bioethanol production. The nitrogen content of biomass and associated N_2O release from biofuels should be of high relevance for the selection of useful biofuel sources and components.

2.3. Considerations for Useful Biofuels

To achieve greenhouse-gas reduction by substituting biofuels for gasoline, the carbon benefits must balance the carbon costs over long time periods. Depending on the particular strategy, the outcome can be positive or negative. Searchinger et al.[5] have reported that corn-based ethanol grown in the USA, for example, is likely to almost double greenhouse emissions over 30 years and may continue to contribute to increased greenhouse-gas levels over 167 years. Similar considerations have recently motivated a group of US scientists[6] to identify key aspects that should be observed in the choice of "beneficial biofuels". They advise that "biofuels should receive policy support as substitutes for fossil energy only when they make a positive impact on four important objectives: energy security, greenhouse-gas emissions, biodiversity, and the sustainability of the food supply".[6] Options to meet these criteria are suggested and include the use of native perennial plants or adapted plant mixtures on degraded, nitrogen-poor soils, or abandoned farmlands, an approach discussed earlier by Tilman et al.[7] Such strategies have the potential to generate much larger reductions in greenhouse-gas emissions than obtained when replacing fossil fuels by corn-grain ethanol or soy-bean biodiesel. As shown in Figure 1, this approach may also be regarded as advantageous

Katharina Kohse-Höinghaus is Professor of Physical Chemistry at Bielefeld University. Her research focuses on combustion chemistry and laser analysis of reacting systems. She has served as the President of the Bunsen Society and is President-Elect of the International Combustion Institute. In 2008 she was elected to the National Academy of Sciences Leopoldina and in 2007 she received the Cross of the Order of Merit of the German Federal Republic.

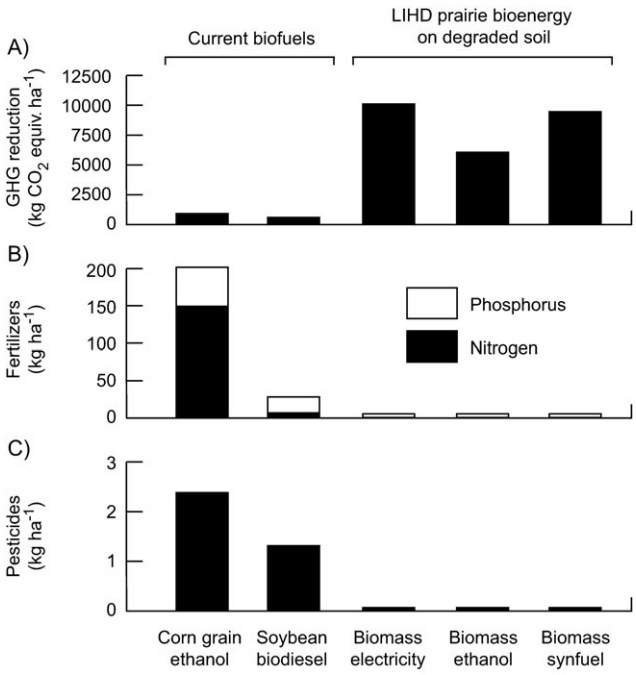

Figure 1. Environmental effects of bioenergy sources. A) Greenhouse gas (GHG) reduction for complete cycles from biofuel production through combustion, showing the reduction in emissions relative to the emissions from the combustion of the fossil fuels which a biofuel substitutes. Average application (in the USA) of B) fertilizer and C) pesticide, for corn and soybeans (from Ref. [29] in Ref. [7]). LIDH: low-intensity high-diversity biomass. From Ref. [7]. Reprinted with permission from AAAS.

with respect to nitrogen and phosphorus content of the biofuel source material. The biofuels from such matter might thus be poorer in fuel-bound nitrogen, a parameter of influence for their combustion emissions.

2.4. Fuel Production from Biomass

Making fuels from biomass is an active field of research, involving chemical engineering as well as biotechnology. Different strategies have been recommended,[8] including hybrid thermochemical and enzymatic approaches[8a] to produce the small, carbon-rich molecules of typical fuels from the long carbohydrate chains encountered in plant matter. Processes can profit from recent advances in chemical catalysis[8b] and the biological engineering of proteins, cells, and metabolic pathways. Identifying more active enzymes and suitable microbes may eliminate critical and energy-costly steps in the biofuel production process.[9] Novel, non-fermentative pathways to biofuels with useful properties have recently been suggested, including higher alcohols, such as butanols.[10] It is thus an intriguing question as to which biofuels will be advocated and available ten years from now.

2.5. Predicting the Combustion Chemistry of Biofuels

From the combustion perspective, the chemical decomposition and oxidation pathways of current and future biofuels are intimately coupled to the structure of the respective fuel molecule. Predicting the combustion behavior of these fuels, including ignition, extinction, heat release, and the formation of potential pollutants, requires the development of detailed combustion mechanisms. These must include all pertinent species, reactions, rate coefficients, and related thermochemical and transport parameters as functions of temperature and pressure. Combustion models which are validated with reliable experiments are used to examine all important aspects of the combustion performance and to transfer the results from the laboratory to the industrial process.

While decades of research has been performed to provide such chemical databases for the conventional hydrocarbon fuels, the experience with the richer chemistry of oxygenated and other bio-derived fuels is comparatively recent. The combination of chemical functional groups in a biofuel molecule may yield reaction sequences not encountered in fossil-fuel chemistry. Important information to anticipate a fuel's combustion properties—including pollutant formation—may thus be lacking. As one example of the detailed chemistry involved, Figure 2 shows some intermediates and

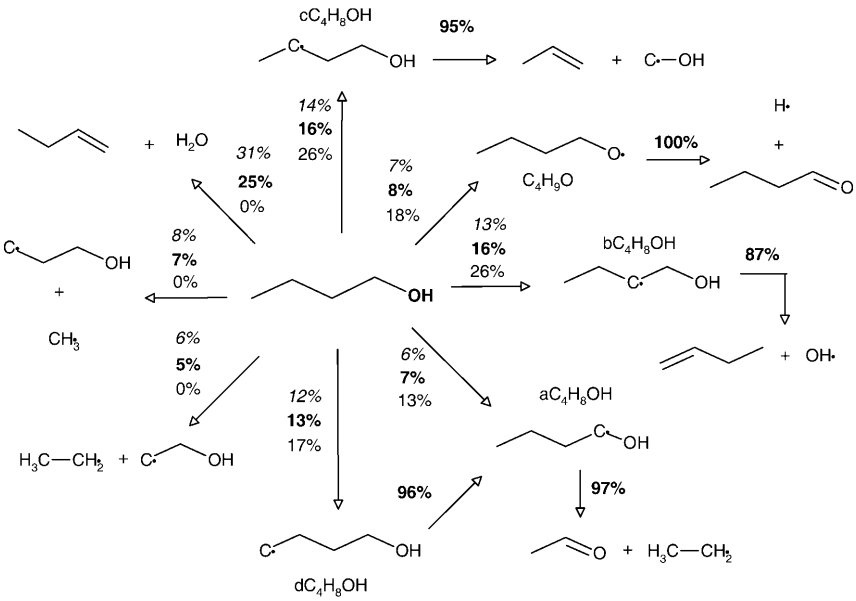

Figure 2. Reaction-pathway diagram for *n*-butanol oxidation in a jet-stirred reactor at $\Phi = 0.5$ (normal text), $\Phi = 1$ (bold text), and $\Phi = 2$ (italicized text). Pressure $p = 1$ atm, residence time $\tau = 0.07$ s, temperature $T = 1160$ K. Reprinted from Ref. [11], with permission from The Combustion Institute.

products in *n*-butanol[*] combustion.[11] From the percentages indicated, it is seen that for comparable experimental conditions (e.g. reactor type, pressure, temperature) the partition between different reaction channels depends on the flame stoichiometry (equivalence ratio Φ).[**] Similar detailed analyses are desirable for the chemical families of typical biofuels, including alcohols, ethers, and esters. Herein, for selected biofuel compounds, we will discuss their combustion reaction sequences and the influence of the structural features of the fuel molecule on intermediates and products, including potential pollutants. Such information is urgently required to assist the evaluation of their suitability as replacement fuels.

3. Combustion-Chemistry Analysis

Combustion is a complex process that generates heat and involves many free-radical species and reactive intermediates in chain-branching, chain-propagation, and termination reactions. For a reliable prediction of the combustion and emission characteristics of a specific fuel, it is not sufficient to provide global parameters, such as octane ratings or ignition delays. To assess pollutant formation, quantitative chemical information is needed, including the nature and amount of undesired and potentially harmful products. These species are not always formed along the main oxidation pathways, and suitably reduced kinetic parameters, adapted to the specific combustion environment, must be derived from more complete combustion models. Computer models that describe the pertinent chemical reaction sequences may involve hundreds of species and reactions. Different environments exist to study aspects of combustion, but to reveal chemical details, it is useful to avoid the complex flow fields of turbulent combustion. High-temperature reaction rate coefficients are often determined in shock-tube experiments. A single elementary reaction—or a subset of reactions from a larger mechanism—can be studied under these conditions, and branching ratios between different product channels can be determined. Reaction-rate expressions from experiments are complemented with information on energy barriers and transition-state configurations from theoretical methods. A reaction mechanism which includes the relevant chemical reactions is compiled for a specific fuel—or a family of similar fuels—and simulation results have been subsequently compared to experimental data from flow reactors, jet-stirred reactors (JSRs), rapid compression machines (RCMs), laboratory flames in different configurations, and from practical combustion systems, obtained using a large arsenal of analysis techniques. Recent advances in combustion kinetics, both from theory and experiment, in combustion diagnostics and combustion modeling have been reviewed in a suite of articles[12–15] which provides a useful introduction into these subjects.

To investigate the flame structure of prototypical biofuel compounds, laminar premixed flames have usually been studied. The flames are typically stabilized on a porous-plug burner at reduced pressure (of typically 50 mbar) to widen the reaction zone where many of the intermediates are formed and consumed. Operated at suitable conditions, this configuration ensures spatial homogeneity across the burner diameter. The combustion progress can thus be described in one dimension (the distance from the burner) from the fresh fuel–oxidizer mixture, through the reaction zone, to the burnt gases where equilibrium is reached. For a hydrocarbon–air flame burning a stoichiometric mixture, the composition in the burnt-gas region consists mainly of the appropriate number of equivalents of CO_2 and H_2O, diluted by N_2. Further main products include oxygenated species and unconsumed O_2, especially for oxygen-rich mixtures ($\Phi < 1$), and CO, H_2, and some hydrocarbons, especially for fuel-rich conditions ($\Phi > 1$). From a chemical, environmental, and public-health perspective, minor products including NO_x, polycyclic aromatic hydrocarbons (PAHs), and soot may be of crucial importance. Much of the existing knowledge on combustion chemistry pertains to flames of aliphatic hydrocarbons, such as alkanes, alkenes, and their cyclic counterparts.[12,16]

Detailed information on flame temperature, qualitative species composition, and quantitative concentrations of reactants, products, stable and reactive intermediates are typically obtained from a combination of methods. These experiments include laser-based measurements, for the temperature profile and small stable and radical species (typically with 2–4 atoms),[15] and different variants of molecular-beam mass spectrometry (MBMS).[17] Mass-spectrometric analysis, often using electron ionization (EI), is advantageous in some respects over laser-based experiments, especially because no prior knowledge of species composition is needed. Exciting recent advances have been made possible by flame-sampling MBMS instruments based at synchrotron light sources that use tunable vacuum-ultraviolet (VUV) radiation for photoionization (PI). Such experiments in the USA[17a] and China,[17c] pioneered by some of the authors and others, allow the unambiguous identification of isomers,[17–19] which is of great value for the investigation of complex reactive environments. Figure 3 illustrates analysis of a dimethyl ether (DME) flame with the PI-MBMS instrument at the Advanced Light Source in Berkeley. A sample is withdrawn from the flame by a quartz cone, expanded into vacuum and ionized by VUV light. The photoions are detected by time-of-flight mass spectrometry. The photon energy is tuned in the appropriate region (8–17 eV) to match the ionization energies of the different chemical species in the sample. A 3 m monochromator provides an energy resolution of < 50 meV, which allows most isomers to be distinguished. However, all sampling techniques inevitably perturb the flame to some extent, and care must be taken to quantify and minimize such influences.[20]

While the PI-MBMS technique is also beneficial for flames of fossil hydrocarbon fuels, it is invaluable for the

[*] Nomenclature for chemicals follows the use in the original literature.
[**] The stoichiometry (equivalence ratio Φ) is used to describe a specific fuel/oxygen ratio compared to the fuel/oxygen ratio needed for complete oxidation to CO_2 and H_2O. In a stoichiometric flame $\Phi = 1$, in fuel-rich flames $\Phi > 1$, and in oxygen-rich flames $\Phi < 1$.

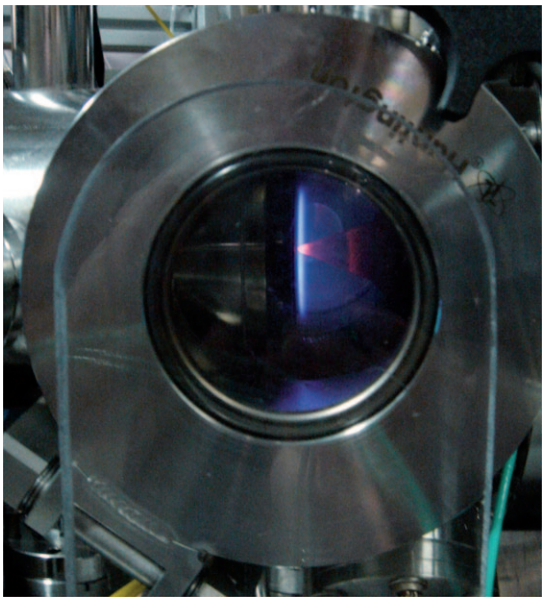

Figure 3. Flame analysis with photoionization molecular-beam mass spectrometer. The geometry is tailored to support a one-dimensional flame where the combustion process can be followed from the fresh gases near the burner surface (left) to the burnt gas (right). Flame gases as a function of position are sampled (such as in this case from the luminous reaction zone) using a quartz cone (right), expanded into vacuum and guided into the ionization chamber coupled to a time-of-flight mass spectrometer.

analysis of the chemistry of biofuel combustion, where isomeric intermediates are especially important as a consequence of the additional chemical functional groups in the fuel molecule. For example, abstraction of any hydrogen atom from ethane (by radicals in the flame) will only produce C_2H_5 radicals. Because of the presence of the hydroxy group in ethanol, the six hydrogen atoms in the molecule are no longer equivalent, and a similar initial fuel-decomposition step yields three different isomeric radicals, CH_2CH_2OH, CH_3CHOH, and CH_3CH_2O.[*] These intermediates will then give rise to different further reaction sequences. In more complex situations than in this simple example, the combination of different laser-diagnostic methods and of MBMS experiments using different ionization techniques is a prerequisite for a reliable analysis of pertinent reaction pathways.

Isomers may not only play an important role as intermediates in combustion chemistry, but potential fuels may themselves come in different isomers. Examples include 1-propanol/2-propanol or the four isomers of butanol. Studies of flames of isomeric fuels can be used to unravel their isomer-specific combustion chemistry and to focus on the influence of the molecular fuel structure on the flame composition.

These and other experimental strategies typically provide data sets that reflect the chemical reaction network in a flame. Valuable information is revealed on the nature of intermediates and products, on their absolute concentrations, and on their formation and consumption profiles along the reaction path. To improve detailed knowledge of reaction sequences, such experimental datasets are compared with computer simulations based on plausible reaction mechanisms. This procedure is invaluable to identify missing links, to test concepts, and to develop a detailed, step-by-step understanding for the entire complicated combustion process.

In a first approach, it is wise to discriminate between bio-derived fuels for transportation and for stationary power generation. For the former, fuels are typically liquids to blend with or to substitute for gasoline or diesel, and different oxygenates are being discussed for this purpose. For the latter, similar fuels may be used in some processes, for example, biodiesel in stationary gas turbines. In addition, however, solid fuels are considered, for example, biomass co-firing with coal.[21–23] Typical biomass fuel sources, such as wastes and plant matter, may contain many elements besides H, C, and O, including N, S, P, Cl, K, Na, Ca, Mg, Fe, and Si.[24] Starting with moderately complex systems, we thus concentrate on oxygenated fuels and provide some perspectives on the combustion chemistry of H,C,O,N-containing biofuels.

4. Combustion Chemistry of Oxygenated Biofuels

Oxygenated fuels as replacements or alternatives to conventional hydrocarbon transportation fuels must be critically examined from different practical viewpoints. Important aspects include, besides availability and production costs, the energy content, the compatibility with delivery infrastructure (e.g., fuel stations and distribution) and with combustion machinery (e.g., automotive engines and gas turbines). Such considerations are currently discussed in view of fuel properties and advances in combustion concepts.[25–33] Combustion chemistry aspects are involved particularly in ignition, heat release, and extinction processes. They are of paramount influence on the pollutant emission signature. For example, particulate emission can be reduced by addition of ethanol,[27] but undesired aldehyde emissions may then increase significantly.[25] Also, increased emissions from NO_x have been observed from biodiesel combustion.[31] Several variants of oxygenated fuels are currently available from starch, sugar, or oil crops, including bio-alcohols and biodiesel. The biodiesel class of compounds is especially diverse chemically, and to understand implications for the combustion process, it is useful to consider prototypical representatives in systematic laboratory studies.

4.1. Ethanol

Ethanol had a long career as a transportation fuel in the early 20th century, until it was superseded by gasoline;[25] it is now one of the most common and abundant biofuels.[34–36] Figure 4 shows the worldwide fuel-ethanol production in the years 2007 and 2008.[34] The USA and Brazil are by far the world's largest producers of fuel ethanol with about 9 billion and 6.5 billion gallons per year, respectively. Most ethanol

[*] Notation for radical structures follows the common practice in the combustion literature, that is, without indicating the unpaired electron.

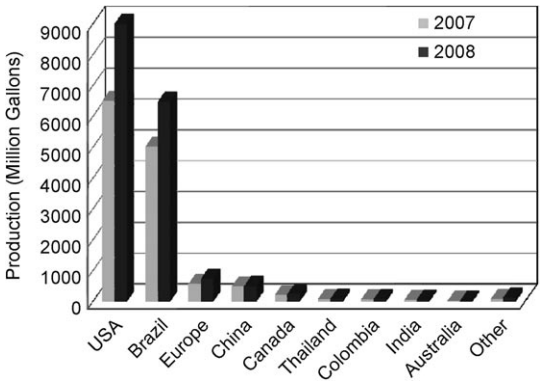

Figure 4. World fuel-ethanol production.[34]

fuel in the USA is made from corn, and ethanol production is increasing.[36] In Brazil, ethanol fuel production from sugar cane has a long tradition.[34,35] The majority of new cars sold there are actually fuel-flexible vehicles which tolerate gasoline–ethanol blends (with typically 20–25 vol% ethanol) as well as pure ethanol.[35] In Europe, sources for bio-ethanol are wheat, sugar beets, and wastes from wine-making with an increasing demand estimated at 12.7 billion liters per year in 2010.[35] Recently established pilot plants are used to investigate the production of cellulosic ethanol to make it commercially viable in the near future.[36]

Ethanol combustion has been studied and modeled in shock-tube, flame, and reactor experiments over wide ranges of temperature and pressure.[37–41] The main reaction sequences, identified by integrating consumption rates for each species over the entire field of a partially premixed ethanol flame are shown in Figure 5.[39] It is useful to analyze this scheme with respect to potential pollutant formation. A primary fuel-decomposition product is ethene, which is also formed via the CH_2CH_2OH hydroxylethyl radical; ethene's further reactions are identical to those encountered in hydrocarbon flames. Final oxidation steps to CO and CO_2 (e.g., from HCCO) are not shown.[39] The other two radicals initially formed by H-abstraction from the fuel will generate acetaldehyde (ethanal, CH_3CHO), a hazardous air pollutant. Also, production of formaldehyde (methanal, CH_2O)—another air pollutant—can be rationalized from this scheme through the C–C β-scission of the ethoxy radical, showing how aldehyde emissions may be expected from ethanol combustion.

In a detailed EI- and PI-MBMS study of premixed ethanol flames of different stoichiometry,[42] Kasper et al. have determined quantitative mole fractions of most stable and radical intermediates. To investigate differences to hydrocarbon-combustion chemistry, these mole fractions were compared to those in flames of propene as a representative hydrocarbon fuel.[42] Alkenes are important constituents of fossil fuels, and combustion of propene as a C_3-hydrocarbon forms C_3H_3 radicals easily which are precursors for aromatics and, eventually, soot. Typical intermediate species concentrations in the ethanol flames are given in Figure 6. In the rich flame, all hydrocarbon intermediates are more abundant. Their peak mole fractions are lower, however, than in a

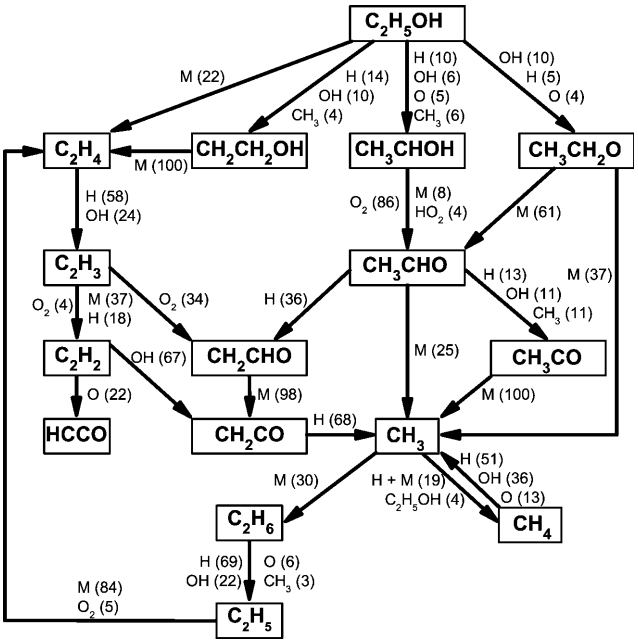

Figure 5. Reaction-pathway diagram for a partially premixed counterflow ethanol flame. Arrows show the main pathways. Next to the arrows, some important reaction partners are indicated with the percentage of their contributions; for example, the reaction of ethanol with OH contributes to 10% to the formation of CH_2CH_2OH. Adapted from Ref. [39], with permission from The Combustion Institute.

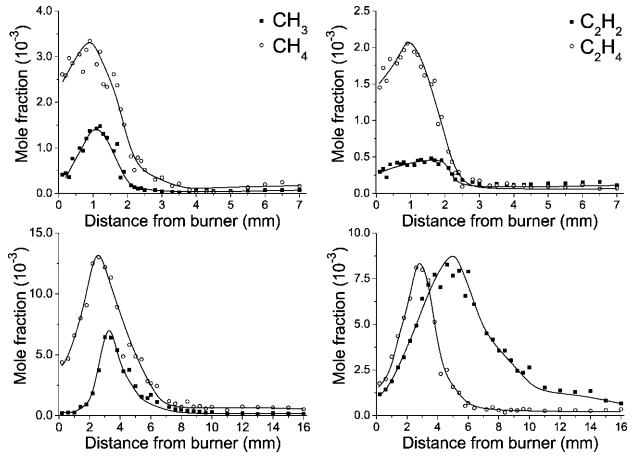

Figure 6. Some intermediate species mole fractions in premixed low-pressure (50 mbar) ethanol–oxygen–argon flames of different stoichiometry. Left: CH_4 (○) and CH_3 (■); right: C_2H_2 (■)and C_2H_4 (○); top: stoichiometric flame with $\Phi = 1$ (C/O = 0.286); bottom: fuel-rich flame with $\Phi = 2.57$ (C/O = 0.600). Adapted from Ref. [42] and reprinted with permission from The Combustion Institute.

corresponding propene flame, as expected for an oxygenated fuel. For example, maximum C_2H_2 mole fractions are 4.8×10^{-4} and 8.3×10^{-3} in the stoichiometric and fuel-rich ethanol flames, respectively, and 3.3×10^{-2} in a rich propene flame.[42] Similarly, C_3H_3 radicals and benzene are factors of 3–20 less important in the rich ethanol flame, respectively, than in a propene flame of comparable stoichiometry. In contrast, mole fractions of oxygenated intermediates are higher in the

ethanol flame than in the propene flame.[42] In the rich ethanol flame, formaldehyde reaches 9.4×10^{-3}, significantly higher than in the corresponding propene flame, and acetaldehyde is of the order of 10^{-3}, whereas it is below the detection limit of a few ppm in the propene flame.[42] From these results, it might be inferred more generally that the combustion of all oxygenates would reduce PAHs and soot precursors but would increase aldehyde concentrations. To understand the influence of the fuel structure more clearly, however, it is instructive to analyze, in similar detail, the combustion chemistry of the ethanol isomer dimethyl ether, a simple oxygenated fuel with C–O but without C–C bonds.

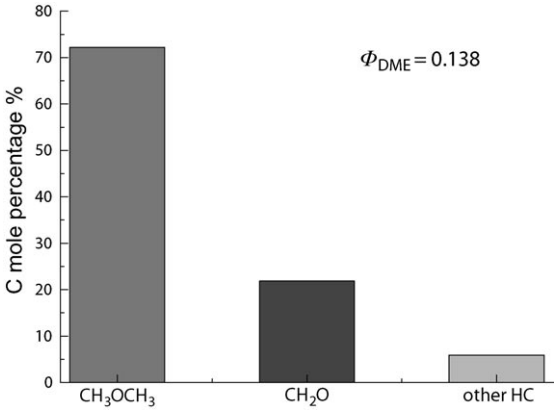

Figure 7. Composition of the unburned hydrocarbon fraction from homogeneous-charge compression-ignition combustion with dimethyl ether fuel ($\Phi = 0.138$). Reprinted from Ref. [47], copyright Elsevier (2009).

4.2. Dimethyl Ether

Ethers, such as methyl *tert*-butyl ether (MTBE), ethyl *tert*-butyl ether (ETBE), and *tert*-amyl methyl ether (TAME), are common octane-improving gasoline additives. In the USA, ground-water contamination by MTBE has led to gradual replacement of this additive with ethanol. Ethers (including ETBE) or alcohols (including methanol and ethanol) are also being recommended to improve diesel combustion.[43–45] Dimethyl ether (CH_3OCH_3, DME), the simplest ether, is a potential alternative to diesel and biodiesel. It has no carbon–carbon bond, a high oxygen content, high cetane number, and low boiling point. Some physico-chemical properties of DME, ethanol, and of conventional hydrocarbon fuels are shown in Table 1. DME can be produced from natural gas, biomass, or coal (via synthesis gas and methanol) and, especially in China, DME is regarded as an attractive alternative transportation fuel.[46,47] It can be used in gas turbines for power generation, for household purposes, and in diesel and homogeneous-charge compression/ignition (HCCI) engines.[47,48] In HCCI combustion, an innovative low-temperature low-emission process, chemical–kinetic aspects play an important role. Recent results show that the emission of unburned hydrocarbons and CO may be a problem associated with DME in HCCI combustion.[47] For the example, in Figure 7, 96.85 % of the DME carbon is converted into CO_2, and 0.71 % into CO; the remaining fraction of 2.44 % that is presented in the figure contains unburned hydrocarbons. This fraction is composed of mostly unburned DME (> 70 % C), a high level of formaldehyde (> 20 % C), and of other hydrocarbons.[47]

Detailed combustion aspects of DME have been studied at ambient and elevated pressure by several authors,[48–53] and kinetic models have been developed.[54–56] Cool et al.[57] and Wang et al.[58] have recently analyzed DME combustion in premixed low-pressure flames using PI- and EI-MBMS. Mole fractions of several intermediates, especially C_1 and C_2 species,[*] are presented in Figure 8.[57] The experimental profiles are shown along with simulations. The shapes of the profiles agree generally quite well, and the largest differences in quantitative mole fractions are only within factors of 2 to 3, permitting an accurate assessment of the importance of various combustion reactions. Intermediates present in appreciable concentrations include CH_4, CH_2O, C_2H_2, C_2H_4, C_2H_6, CH_3OH, and CH_3CHO. Radicals include the chain carriers H, O, and OH (which are involved in H-abstraction reactions and persist throughout the flame) as well as CH_3 and HCO. A reaction-flux analysis[57] reveals that the important reaction sequences are similar to those encountered in propane combustion. This result is not surprising because DME and propane are isoelectronic. As a saturated molecule, DME is decomposed by H-abstraction, yielding CH_3OCH_2, which subsequently decomposes to CH_3 and CH_2O via β-scission (analogous to *n*-propyl reacting to CH_3 and C_2H_4). Formaldehyde is predominantly formed through this reaction. Through recombination reactions, methyl radicals play an

[*] C_1 (C_2, ...,C_n) species: compounds featuring one (two, ..., *n*) carbon atoms.

Table 1: Properties of several oxygenated and conventional fuels; adapted from Ref. [25].

Fuel	Methane	Methanol	Dimethyl ether	Ethanol	Gasoline	Diesel
Formula	CH_4	CH_3OH	CH_3OCH_3	CH_3CH_2OH	C_7H_{16}	$C_{14}H_{30}$
Molecular weight [g mol^{-1}]	16.04	32.04	46.07	46.07	100.2	198.4
Density [g cm^{-3}]	0.00072[a]	0.792	0.661[b]	0.785	0.737	0.856
Normal boiling point [°C]	−162	64	−24.9	78	38–204	125–400
Lower heat value [kJ cm^{-3}]	0.0346[a]	15.82	18.92	21.09	32.05	35.66
Lower heat value [kJ g^{-1}]	47.79	19.99	28.62	26.87	43.47	41.66
Carbon content [wt %]	74	37.5	52.2	52.2	85.5	87
Sulfur content [ppm]	ca. 7–25	0	0	0	ca. 200	ca. 250

[a] Values per cm^3 of vapor at standard temperature and pressure. [b] Density at 1 atm and −25 °C; for sources of reported values see Ref. [25].

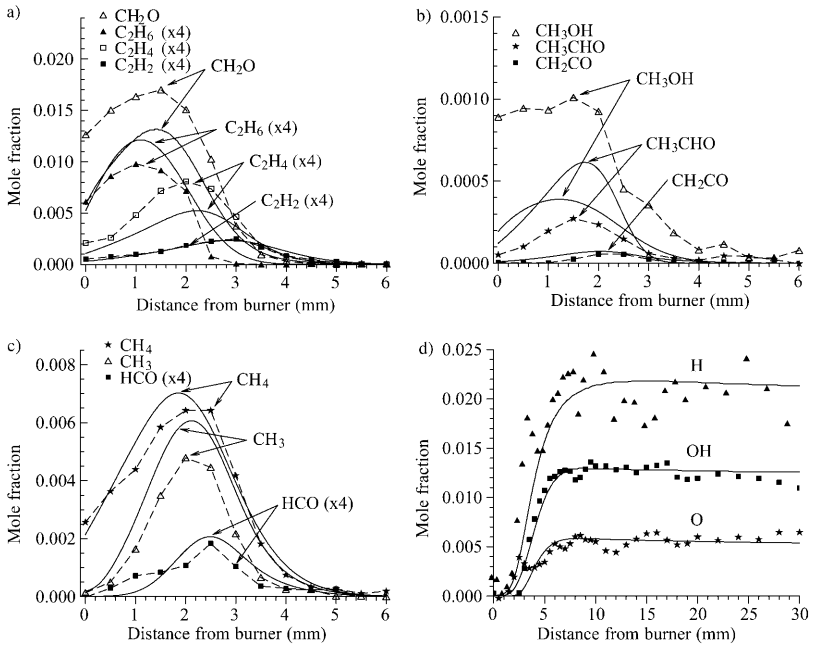

Figure 8. Mole fractions for intermediate and minor species in a premixed low-pressure (40 mbar) dimethyl ether flame of $\Phi = 1.2$; symbols are experimental results, solid lines modeling results. Reprinted from Ref. [57], with permission from The Combustion Institute.

important role in the formation of C_2 species. Final oxidation reactions involve the formyl radical and CO.

Reaction paths and intermediate concentrations also depend on stoichiometry. Changes in formyl and formaldehyde profiles in DME flames from near-stoichiometric ($\Phi = 0.93$) to fuel-rich ($\Phi = 1.86$) conditions are shown in Figure 9.[58] The flame model[56] captures the experimentally observed increase in the formaldehyde mole fraction towards fuel-rich conditions with high accuracy. The mole fraction of CH_2O reaches 1–3%, which is a very large value for any reaction intermediate in typical laminar premixed flames. The agreement of experimental and modeling results for HCO (the mole fraction of which is 10-fold lower), is within the range expected for reactive species. A similar analysis was performed for important C_1 and C_2 intermediates, most of which attain highest mole fractions in the richest flame. Experimental acetaldehyde and methanol mole fractions decrease with increasing equivalence ratio, a trend that is correctly predicted for acetaldehyde but not for methanol. Acetaldehyde is a minor intermediate in the DME flame with almost 100-fold lower mole fractions than formaldehyde,[58] a different relationship to that seen in the corresponding ethanol flames.[42]

A reaction-flux analysis tracing the fate of fuel carbon is given in Figure 10 for the two limiting stoichiometries.[58] It summarizes prominent features discussed before. The most important oxidation route (represented by the thickest arrows) leads through formaldehyde, and the C_2 hydrocarbon sequence, starting from methyl recombination, appears almost decoupled from the main oxidation path. The different relations of formaldehyde and acetaldehyde mole fractions in DME and ethanol flames are consequences of the absence of a carbon–carbon bond in DME and the fact that the carbon–oxygen bond in the fuel molecule remains intact through several reaction steps. Since both fuels have the same oxygen content, this observation illustrates how the intermediate species composition of the combustion process can be influenced by the chemical structure of the fuel.

4.3. Hydrocarbon–Oxygenate Fuel Blends

Current policy for carbon dioxide reduction in several regions of the world is to use mixtures of fossil and biogenic fuels which can replace the neat hydrocarbon fuels without any changes in the respective combustion engine. Ethanol and ethers can be blended or added to hydrocarbon fuels to improve combustion.[47,59–61] Interactions of the reactive intermediates from all components in such fuel

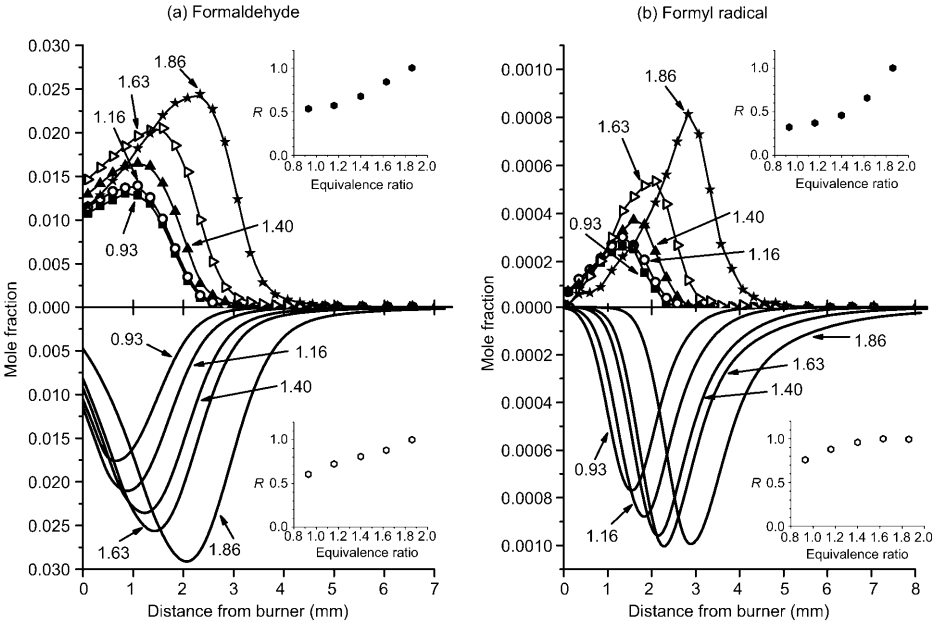

Figure 9. Comparison of measured (top panels) and calculated (bottom panels) mole-fraction profiles for a) formaldehyde and b) formyl radical in premixed dimethyl ether flames (33 mbar) of different stoichiometry ($\Phi = 0.93$, 1.16, 1.40, 1.63, and 1.86). The insets show the measured (top) and predicted (bottom) variations in peak mole fractions as a function of equivalence ratio; *R*: ratio of peak mole fraction.[58] Reproduced by permission of the PCCP Owner Societies.

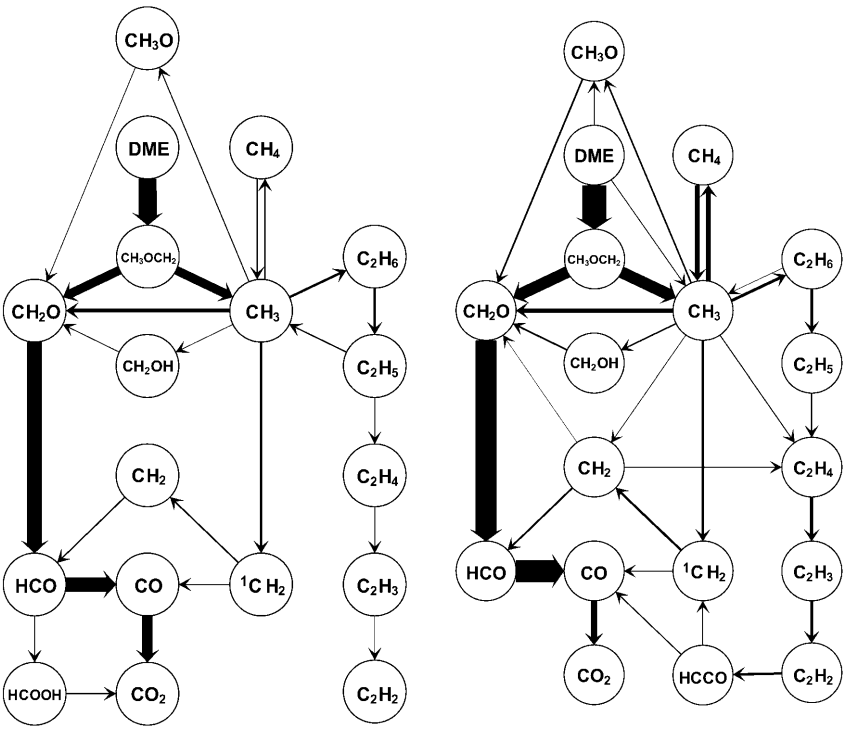

Figure 10. Reaction pathways in premixed dimethyl ether–oxygen–argon flames (33 mbar) of $\Phi = 0.93$ (left) and $\Phi = 1.63$ (right). The thickness of the arrows encodes the reaction flux: values are integrated over a zone of 0–10 mm above the burner and normalized to the largest flux of 5.05×10^{-5} mol cm^{-2} s^{-1} for $CH_3OCH_3 \rightarrow CH_3OCH_2$ in the $\Phi = 1.63$ flame. Paths with fluxes of $< 2\%$ of this value are not shown.[58] Reproduced by permission of the PCCP Owner Societies.

blends may have consequences for combustion emissions.[62,63] Chemical effects of oxygenate addition to hydrocarbon combustion have been investigated in detailed studies in flames and reactors.[64–72] For example, DME addition to methane may enhance ignition by rapidly forming CH_3 and HO_2 radicals, which promote faster chain propagation.[69] The combustion behavior of E10 and E85 mixtures[*] for fuel-flexible vehicles was illustrated in a jet-stirred reactor with blends of ethanol and *n*-heptane.[70] The experimental mole-fraction profiles in Figure 11 for a 50:50 mol% mixture at 10 atm were simulated with a model that merges alkane and ethanol combustion chemistry. This mechanism involves 564 species and 2589 reactions and describes the experiment with respectable agreement. Fuel consumption starts above 800 K; intermediates involve H_2, hydrocarbons, and aldehydes; and conversion into CO_2 and H_2O proceeds near 1100 K. Distinct zones reflect the typical regions of cool-flame, negative-temperature-coefficient, and high-temperature behaviors.[**] The model reveals decomposition and oxidation reactions of both fuels and their interaction. Ethanol alone would not oxidize through a cool-flame mechanism, but decomposition of *n*-heptane provides the necessary radicals in this low-temperature region.[70] Regarding potential pollutant emissions with increasing ethanol content of the fuel, acetaldehyde is increasingly formed by oxidation of CH_3CHOH.[70]

The importance of chemical interactions in fuel blends is especially evident when isomeric oxygenated additives, such as DME and ethanol, are compared by mixing each into a flame of the same hydrocarbon fuel. A modeling study adopting this strategy[65] concentrates on soot-precursor formation in fuel-rich alkane combustion, where oxygenate addition may reduce soot emission. The model suggests (Figure 12) that the observed cleaner combustion is not only the result of the quantity of oxygen added, but that DME vs. ethanol addition to fuel-rich ethene flames has a chemical effect on the formation of compounds with one to four aromatic rings. This behavior is attributed to the ease of production of critical C_2 species that play a role in the formation of benzene and PAHs.[65] Compared with DME, the C–C bond in the molecular structure of ethanol clearly favors these C_2 pathways.

Differences in concentrations of C_1–C_{12} hydrocarbons and soot upon DME or ethanol addition are reported from experiments in non-premixed ethene flames.[66] Examples are given in Figure 13 for CH_4, C_2H_2, and C_2H_4O, and are discussed in terms of key fuel-decomposition reactions. Pure ethene combustion ($\beta = 0$) results in large C_2H_2, low CH_4, and low C_2H_4O mole fractions. DME addition increases CH_4 mole fractions through CH_3 radicals, but reduces C_2H_2 mole fractions because C_2H_2 is not a product of DME decomposition. The effects on CH_4 production and C_2H_2 reduction are smaller for ethanol, because not all fuel decomposition pathways for ethanol involve CH_3 or ethene (see also Figure 5). The mole fractions of acetaldehyde increase upon ethanol addition, where a direct pathway exists, in contrast to DME, where such a direct production channel is not available[66] (compare Figure 10). Addition of both oxygenates increases mole fractions of benzene, its precursors, and soot, with a slightly larger effect for DME addition. These results, which seem to be in contrast with Ref. [65], were recently confirmed by an experimental and modeling investigation,[71] which reveals more details of the combustion chemistry. For example, oxygenate addition leads to increased levels of C_3H_3, a major benzene precursor, by combination of CH_3 and C_2H_x species; the former is more easily produced with DME, and the latter with ethanol addition. The apparent conflict regarding the effect of oxygenate addition on the formation of soot and its precursors[65,66,71] may be attributed to the different flame configurations, for example, premixed

[*] E10: 10 vol% ethanol, E85: 85 vol% ethanol with gasoline.

[**] In alkane combustion, "cool" flames may occur at temperatures below the minimum autoignition temperature. Combustion is not completed, however, at these low temperatures, but followed by a zone of negative temperature coefficient where the global reaction rate decreases; this is associated with the formation of alkylperoxy radicals. Chain-branching reactions at higher temperatures multiply the number of reactive species which ensure complete oxidation.

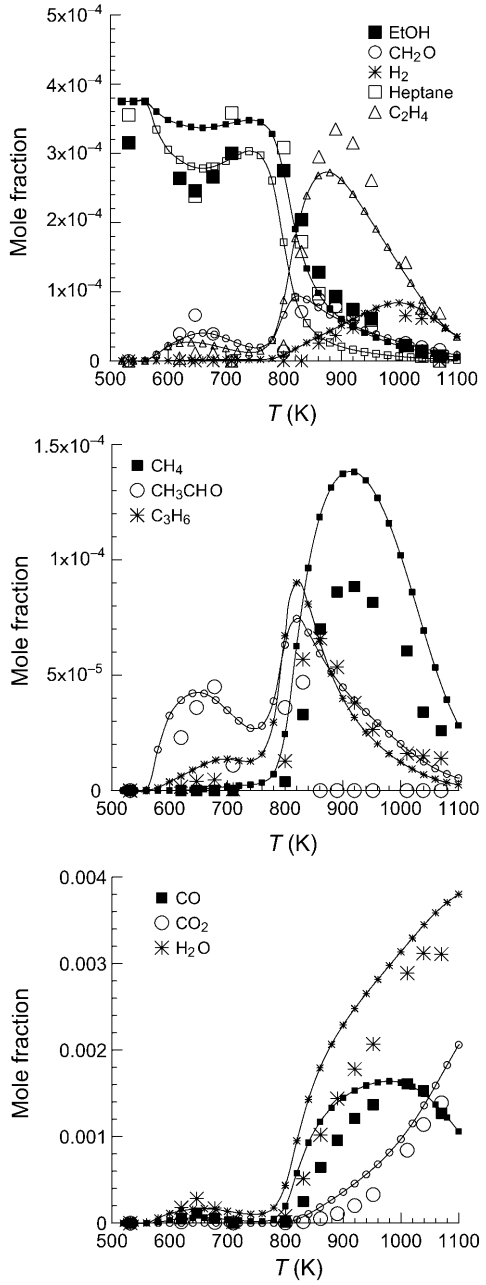

Figure 11. The oxidation of a nitrogen-diluted ethanol–heptane 50:50 mol% fuel mixture in a jet-stirred reactor at 10 atm, 700 ms residence time, and $\Phi = 0.5$. Experimental results (symbols) and detailed modeling (lines and small symbols). Reprinted from Ref. [70], copyright Elsevier (2010).

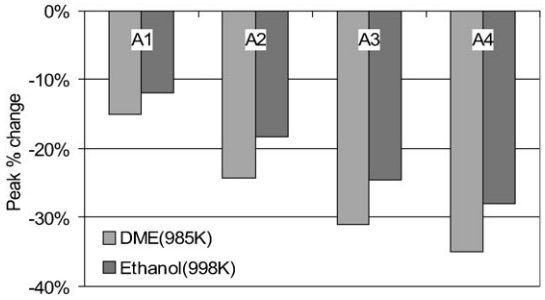

Figure 12. The effect of DME and ethanol (9.9 mol%) on the peak mole fraction of aromatic species with an initial temperature adjusted to give the same final temperature as the reference case (fuel-rich ethane combustion, calculated for a constant-pressure reactor). A1: benzene, A2: naphthalene, A3: phenanthrene, A4: pyrene. Reprinted from Ref. [65], with permission from The Combustion Institute.

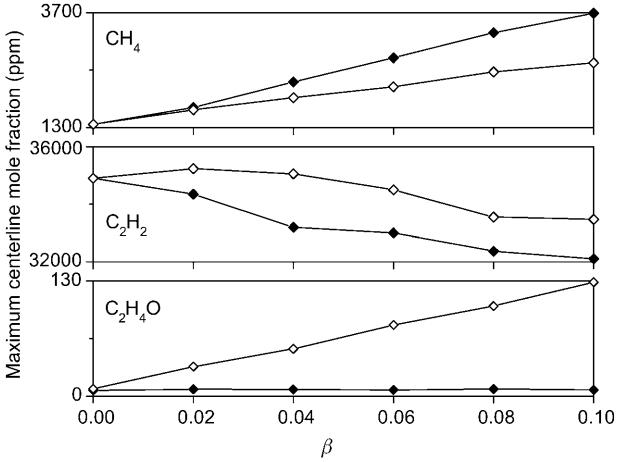

Figure 13. Maximum centerline mole fraction of CH_4 (methane), C_2H_2 (acetylene), and C_2H_4O (acetaldehyde). Filled symbols: DME–C_2H_4 flames; open symbols: ethanol–C_2H_4 flames. β is the ratio of the volumetric flow rates of oxygenate and ethene fuels. Reprinted from Ref. [66], with permission from The Combustion Institute.

versus non-premixed flame structure. This effect was demonstrated when ethanol was added to the air stream rather than to the fuel in non-premixed ethane flames.[72] Formation of soot decreased in the former, and increased in the latter case.

In an extensive study focused on the intermediate-species pool, Wang et al.[68] have recently investigated five pairs of propene–ethanol and propene–DME flames with blends ranging from pure propene to pure oxygenate. Similar experiments were conducted for flame sets of additional stoichiometries.[67] The reliability of these experiments is enhanced by comparing identical flame conditions with the two independent EI- and PI-MBMS instruments and by using identical mixture compositions for both oxygenates. A large number of species, including the C_1 to C_6 families, was quantitatively measured in all flames. Figure 14 and 15 provide mole-fraction profiles for C_2 species and aldehydes, respectively. Substitution of propene with both oxygenates reduces mole fractions of C_2 species almost linearly, with a slightly more prominent effect for DME. Numerous hydrocarbon intermediates show a similar trend, including typical benzene precursors and benzene. Mole fractions of only a few species increase when propene is replaced by oxygenate fuel. These increasing species are methanol and HCO with both additives, formaldehyde, CH_3, and CH_4 in the DME-doped flames, and acetaldehyde when ethanol is added. Figure 14 shows that the unsaturated C_2 species are readily formed in the pure propene flame, and replacement by DME has a larger effect on their mole fractions because C_2 compounds are not direct products from DME but require CH_3 recombination. Species with three to six C atoms are characteristic for

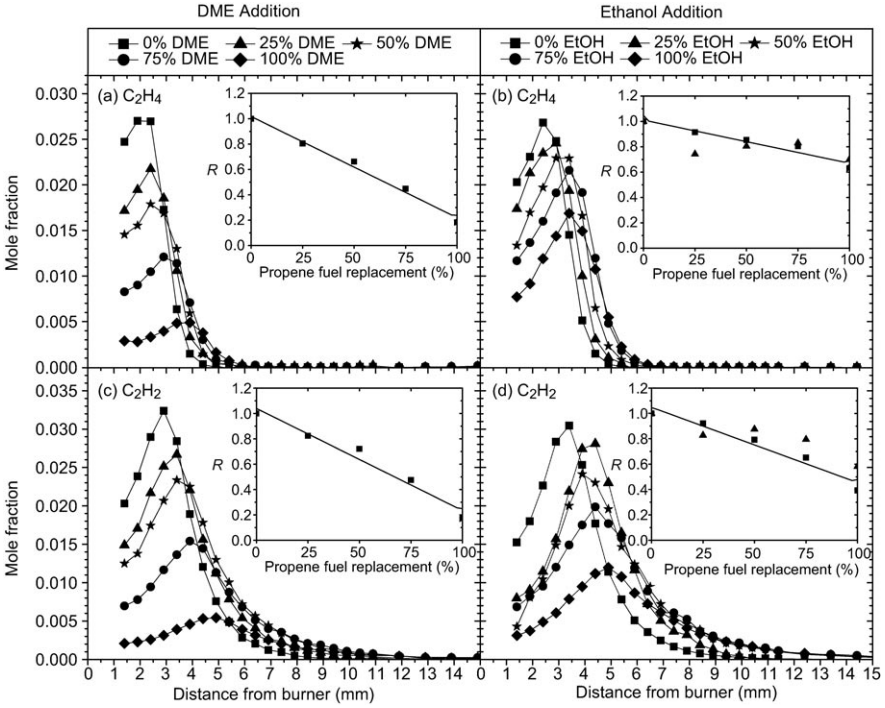

Figure 14. Ethylene and acetylene mole-fraction profiles for dimethyl ether–propene and ethanol–propene fuel mixtures (premixed flames with C/O ratio of 0.5 at 40 mbar). The inserts show the measured peak mole fractions relative to those of the propene flame (0% additive); *R*: ratio of peak mole fraction. Reprinted with permission from Ref. [68]. Copyright 2008 American Chemical Society.

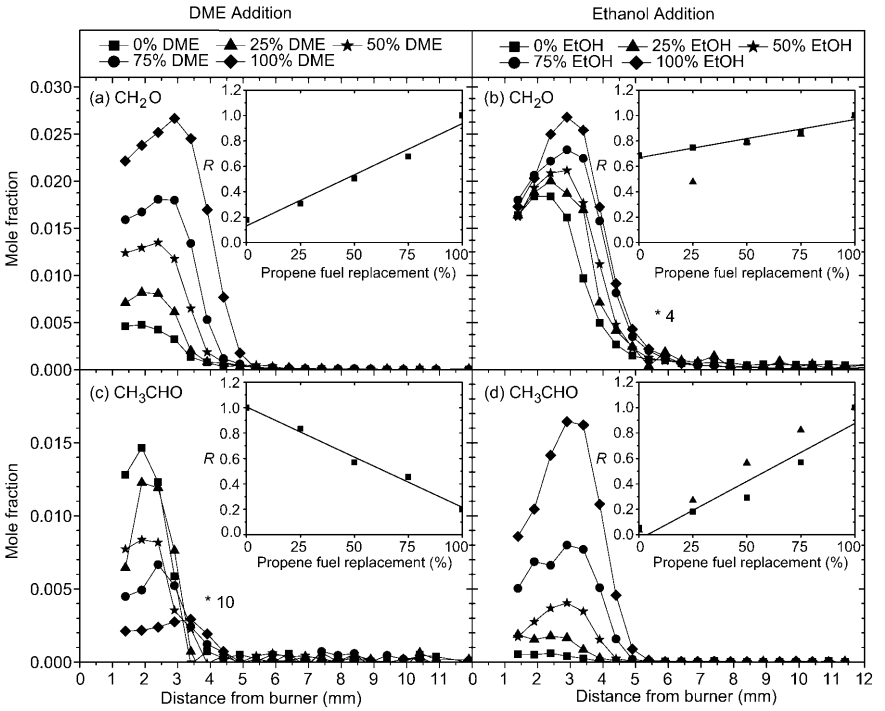

Figure 15. Formaldehyde and acetaldehyde mole-fraction profiles for dimethyl ether–propene and ethanol–propene fuel mixtures (premixed flames with C/O ratio of 0.5 at 40 mbar). To facilitate comparison, all mole fractions are multiplied by a factor of 4 in panel (b) and by a factor of 10 in panel (c); *R*: ratio of peak mole fraction. Reprinted with permission from Ref. [68]. Copyright 2008 American Chemical Society.

rich propene combustion, and their identities and quantities are similar for both additives. The results for CH_2O and CH_3CHO in Figure 15 show a strong dependence on the respective fuel blend. Both additives increase formaldehyde mole fractions, with a stronger effect for DME–propene mixtures. Acetaldehyde mole fractions decrease with DME substitution of propene but increase upon ethanol addition. CH_2O mole fractions are higher for DME-containing fuels, and CH_3CHO levels are higher for the corresponding ethanol–propene mixtures. These observations can be understood from the detailed reaction schemes (Figures 5 and 10), involving characteristic decomposition steps and intermediates, for example, CH_3OCH_2 forming $CH_3 + CH_2O$ upon DME addition and CH_3CHOH reacting to give $CH_3CHO + H$ in the ethanol mixtures.[68]

These rather simple examples demonstrate the complexity of the combustion of hydrocarbon–oxygenate blends; trends depend intimately on specific features of the fuel molecules and on combustion conditions. Further experimental and modeling efforts are needed to conceive minimal pollutant emission strategies, especially because PAHs and soot on the one hand and oxygenated pollutants on the other are affected in opposite directions. Current models capture general decomposition and oxidation behavior for some oxygenate fuels and fuel blends reasonably well; however, a large influence must be attributed to some pivotal reactions generating important chain carriers. Reliable predictions of pollutants require improved chemical–kinetic information for such species to be determined from experiment and theory.[73,74]

4.4. Propanol

Propanol exists in two isomers: 1-propanol ($CH_3CH_2CH_2OH$) and 2-propanol ($CH_3CHOHCH_3$). Both isomers of propanol can be produced as potential alternative fuels from biomass.[75] Furthermore, propanol com-

bustion reactions are a subset of those of butanol. Detailed studies of the combustion of propanol and other oxygenated C_3 fuels, including acetone and propanal, have become available.[76–80] In the exhaust of engines fueled with a hydrocarbon–oxygenate blend containing 2-propanol, high concentrations of acetone were detected, confirming that carbonyl compounds are indeed common products of alcohol—not only ethanol—combustion.[81] Comparing identical 1-propanol and 2-propanol flames can elucidate influences of the fuel's molecular structure on the reaction pathways and species composition.

A destruction scheme for both fuels, assuming H-abstraction and β-scission reactions common to high-temperature combustion as initial fuel decomposition steps, is presented in Figure 16.[76] Substantial differences are evident and were

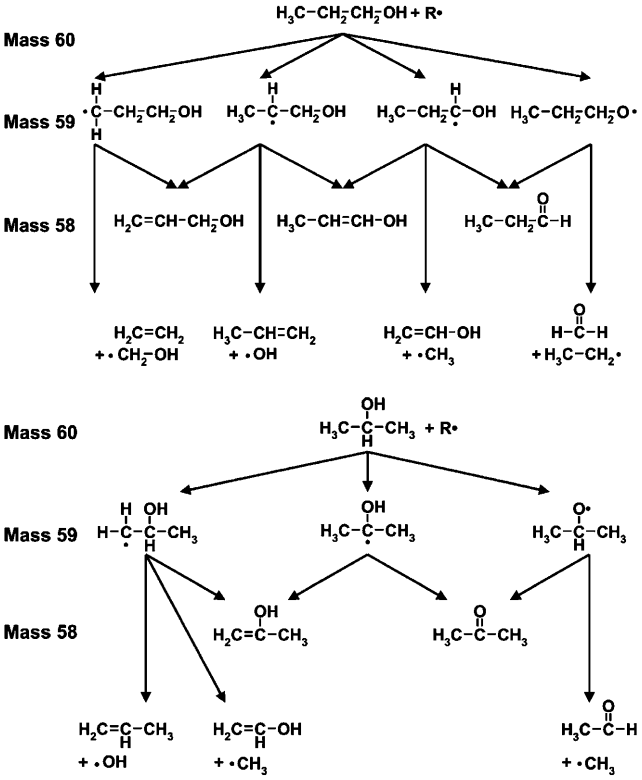

Figure 16. Probable intermediates produced in the first fuel destruction steps in 1-propanol flames (top) and 2-propanol flames (bottom). Reprinted from Ref. [76], with permission from The Combustion Institute.

corroborated by EI- and PI-MBMS experiments.[76] Initial reactions yield four radicals of mass 59[*] for 1-propanol and three for 2-propanol. The first four radicals can react further to 1-propenol, 2-propen-1-ol, and propanal as major products at m/z 58, and the latter three radicals to acetone and propene-2-ol. The identification of isomers and near-equal-mass species is demonstrated in Figure 17 for the signal at

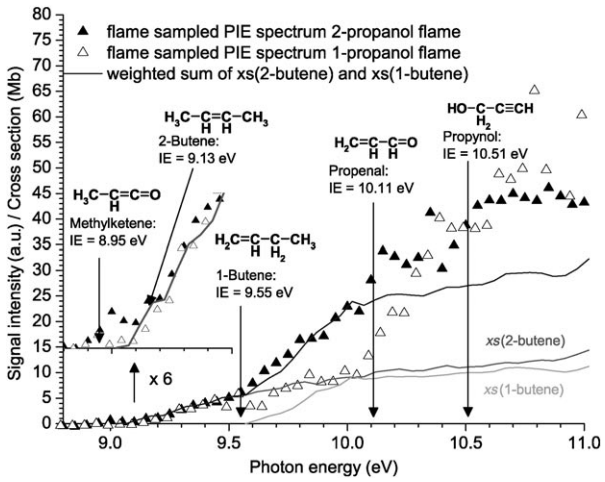

Figure 17. Flame-sampled photoionization efficiency (PIE) curves (m/z 56) from fuel-rich ($\Phi = 1.9$), premixed 1-propanol (△) and 2-propanol (▲) flames (47 mbar) and the PIE curves of 1- and 2-butene. In the range up to 10.10 eV, experiments are matched assuming the 2-butene cross section in the 1-propanol flame and a weighted sum (40:60) of the ionization cross sections of 2-butene and 1-butene in the 2-propanol flame. Reprinted from Ref. [76], with permission from The Combustion Institute.

nominal m/z 56. Several C_4H_8 and C_3H_4O compounds are conceivable, and their separation was possible with the PI-MBMS instrument. The ionization energies are indicated for methylketene, 2-butene, 1-butene, propenal, and propynol. The presence of 2-butene and propenal was confirmed for both propanol fuels, and 1-butene (see onset at 9.55 eV) was detected in 2-propanol flames.[76] Methylketene was reported to be present in lean (that is, oxygen-rich) 1-propanol flames.[78] The higher mass resolution of the EI-MBMS instrument allowed for contributions from C_4H_8 (56.062 g mol^{-1}) and C_3H_4O (56.026 g mol^{-1}) to be resolved by their mass-to-charge ratio. Mole fractions were determined as a function of stoichiometry for a large number of intermediates. Distinct differences are observed for oxygenates: CH_2O, CH_2OH, CH_3O, CH_3CHO, and C_2H_3OH dominate for 1-propanol flames and acetone for 2-propanol flames. Propane is only found in 1-propanol flames.

Features of the combustion of acetone, a component in the acetone–butanol–ethanol (ABE) fermentation process,[82] have been compared with those of the combustion of the propanol isomers.[78] Example photoionization efficiency (PIE) spectra in Figure 18 show the contributions of ethenol and acetaldehyde at m/z 44 and of ketene and propene at m/z 42. Compositions are fuel dependent, with ethenol fractions in the 1-propanol flames exceeding those for 2-propanol and acetone fuels. Many features of acetone combustion are similar to those of 2-propanol because acetone is a direct dehydrogenation product of 2-propanol. Also, the functional group is at the same carbon atom, and both molecules have a symmetric structure with respect to the two methyl groups. Propene can be formed directly by fuel decomposition in 2-propanol flames, but not in acetone flames. Ketene is easily formed from acetone by the reaction $CH_3COCH_2 \rightarrow CH_2CO + CH_3$.

[*] In the MBMS experiments, species were identified according to their mass-to-charge (m/z) ratio and detected as positive ions; notation shows the neutral species in the flame in line with common practice in the literature.

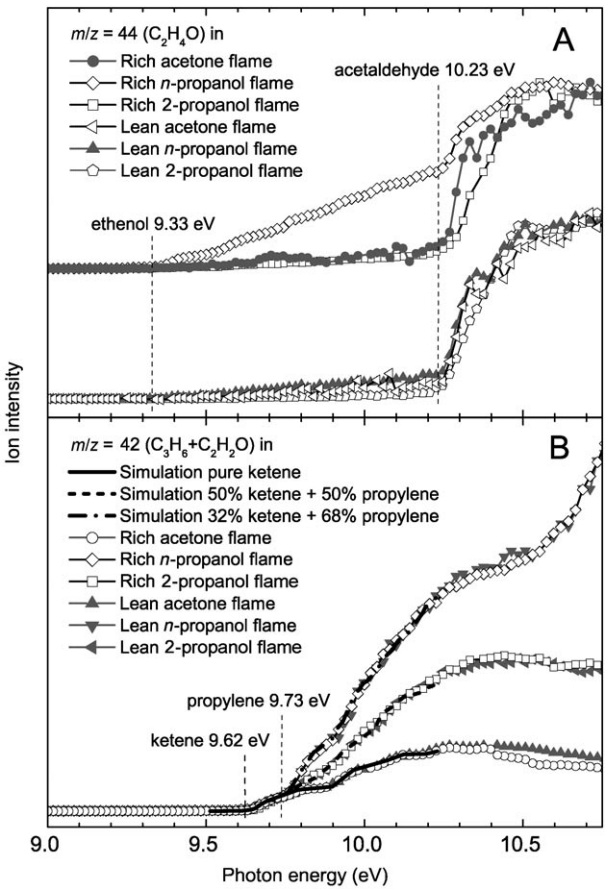

Figure 18. A) PIE spectra of mass 44 (C_2H_4O) measured in rich ($\Phi = 1.8$) and lean ($\Phi = 0.75$) premixed acetone, *n*-propanol and 2-propanol low-pressure flames. B) PIE spectra of mass 42 ($C_3H_6 + C_2H_2O$) measured in the same flames. The literature ionization energies for species identified by the observed ionization thresholds are indicated. Reprinted from Ref. [78], with permission from The Combustion Institute.

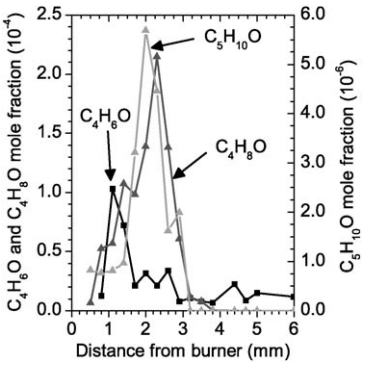

Figure 19. Mole-fraction profiles of C_4H_6O, C_4H_8O, and $C_5H_{10}O$ from a premixed, 50 mbar propanal flame ($\Phi = 1.0$). Reprinted from Ref. [79], with permission from The Combustion Institute.

In addition to the intermediate-species pool observed for ethanol and DME flames where C_1 and C_2 compounds were dominant, higher C_xH_yO species are detected in C_3 oxygenate fuel combustion (Figure 19), including C_4H_6O, C_4H_8O, and $C_5H_{10}O$ from propanal flames.[79] C_4H_8O could be composed of butanone, butenols, and unsaturated or cyclic ethers, such as tetrahydrofuran (THF), the combustion of which is under investigation as a prototype for such compounds.[83] In contrast to carbon build-up reactions preceding soot, the chemistry leading to higher-mass oxygenated compounds in flames is less well known. Recent modeling investigations have provided a mechanism for propanol combustion that reproduces key features of several experiments.[77]

As one approach to identify more general trends in combustion emissions, Table 2 summarizes maximum mole fractions of potential pollutants in flames of different fuels.[78] Although stoichiometries differ for the presented flame data and uncertainties of the absolute values can be substantial, the study suggests that hydrocarbon fuels may produce more toxic hydrocarbons, such as 1,3-butadiene, and oxygenate fuels may produce more toxic oxygenates including aldehydes, ketones, and methanol.[78] Concentrations of these undesired species depend crucially on the chemical nature of the fuel under comparable combustion conditions. With the increasing size of the hydrocarbon or oxygenate fuel, the number of possible reactions becomes larger, and such generalized relations must be examined with caution.

4.5. Butanol

Bio-butanol is a promising fuel candidate that offers several advantages over ethanol, including higher energy content, lower water absorption, better miscibility with present fuels, and unproblematic use in conventional engines.[84] Making bio-butanol is an active field of research[10,75,82,85–87] that dates back to the 19th century. Microbial butanol production was reported by Louis Pasteur and applied industrially by Chaim Weizmann.[85] Depending on the specific biotechnological process, 1-butanol or *iso*-

Table 2: Comparison of the peak mole fractions of major hydrocarbon and oxygenate toxics (rows) between rich hydrocarbon and rich oxygenated flames (columns). Sources for the reported values are given in the original paper.[78]

Fuel → Species↓	Propene	Propane	Benzene	Acetone	1-Propanol	2-Propanol	Methyl acetate	Ethyl formate
1,3-Butadiene	2.4×10^{-3}	4.0×10^{-4}	1.5×10^{-3}	1.3×10^{-4}	9.1×10^{-5}	1.4×10^{-4}	2.8×10^{-5}	1.1×10^{-4}
Formaldehyde	3.7×10^{-3}	3.0×10^{-3}	2.3×10^{-3}	3.0×10^{-4}	6.9×10^{-3}	2.8×10^{-3}	1.6×10^{-2}	4.4×10^{-3}
Methanol	–	3.4×10^{-4}	–	2.8×10^{-3}	8.1×10^{-4}	2.9×10^{-4}	3.8×10^{-3}	5.2×10^{-4}
Acetaldehyde	4.2×10^{-4}	2.6×10^{-4}	–	1.2×10^{-3}	5.2×10^{-3}	1.1×10^{-3}	2.7×10^{-4}	3.9×10^{-3}
Methyl ethyl ketone	–	–	–	1.4×10^{-3}	1.2×10^{-5}	4.2×10^{-5}	–	–

butanol[*] may be obtained.[10,75,87] The branched-chain alcohols feature higher octane numbers. Lignocellulosic materials, such as domestic and fibrous agricultural waste can be used in the ABE fermentation process.[86]

Combustion studies on butanol are receiving increased attention.[88–91] The four structural isomers (1-butanol, 2-butanol, *iso*-butanol, and *tert*-butanol) show different ignition and reaction behavior, while global combustion properties including heat release and CO_2 emission are very similar.[88,89,91] Major-species composition and flame-temperature profiles are almost indistinguishable for premixed laminar flames of identical conditions (Figure 20). Stable and reactive

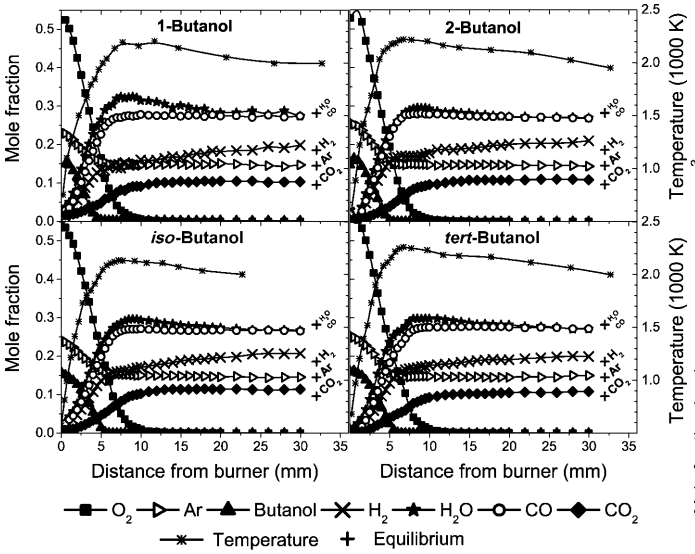

Figure 20. Major-species composition (from EI-MBMS) and temperature profiles (from laser-induced fluorescence of seeded NO) for premixed butanol–oxygen–argon flames at 40 mbar. The four butanol isomers are burned under identical, fuel-rich ($\Phi = 1.71$) flame conditions. Equilibrium mole fractions are indicated at a distance from burner of 32 mm. Independent PI-MBMS results (not shown for clarity) are in excellent agreement.

intermediates depend on the fuel structure and can be understood from the specific early radical attack and decomposition steps.[88,89] Results from shock-tube experiments and modeling indicate that the more reactive 1-butanol and *iso*-butanol are mainly consumed by H-abstraction, and 2-butanol and *tert*-butanol form alkenes by dehydration, accounting for the observed ignition delay times.[91]

A combustion model for 1-butanol has been developed on the basis of jet-stirred reactor and flame experiments.[11,90] Detected species include large amounts of CH_4, CH_2O, C_2H_4, and C_3H_6 and moderate mole fractions of C_2H_6, C_2H_2, and CH_3CHO. Also, 1-butene was found as well as small fractions of butanal, propanal, 2-propenal, and epoxides (oxirane, methyloxirane, and ethyloxirane). The model includes unimolecular decomposition, H-abstraction, β-scission, and isomerization kinetics and captures most experimental trends.[90]

[*] For better legibility regarding the four butanol isomers, the prefix "iso" is not considered as part of the chemical name, contrary to IUPAC recommendation.

Under the experimental conditions, H-abstraction was reported to be the major fuel-consumption pathway, while unimolecular decomposition was relatively unimportant.[90] It is evident from the species composition that progress in the kinetics for smaller alcohols would benefit the development of butanol combustion models. Comparison of 1-butanol and *n*-butane combustion in an opposed-flow diffusion flame shows significant differences for key intermediates.[11] The mole fractions of methane and many C_2 and C_3 species are similar for both fuels, while 1-butanol produces higher amounts of CH_2O, CH_3CHO, C_3H_7CHO, and 1-C_4H_8. As for the smaller oxygenates discussed earlier, the carbon–oxygen bond remains intact during several steps of the fuel destruction process. The observations for 1-butanol can be rationalized with the scheme in Figure 2.

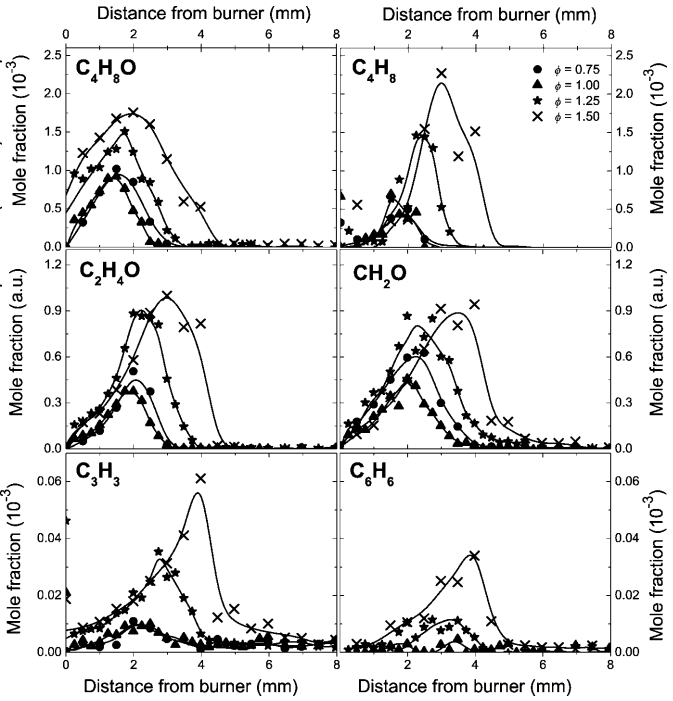

Figure 21. Intermediate-species profiles as a function of stoichiometry for 1-butanol flames. Total mass flow, pressure, and argon fraction match those of the $\Phi = 1.71$ flame in Figure 20.

Some mole fractions of intermediate species determined from EI-MBMS are given in Figure 21 for low-pressure premixed 1-butanol flames of varied stoichiometry. Isomer identification was supported by PI-MBMS measurements. Butanal, ethenol, 1-butene, and hydroxymethylene (CH_2OH), which may decompose to formaldehyde, are products of β-scission from the C_4H_8OH radical with the unpaired electron at the α-, β-, and γ-positions, respectively, and contribute significantly or completely to the C_4H_8O, C_2H_4O, C_4H_8, and CH_2O signals. Also shown are mole fractions of C_3H_3 and benzene as typical PAH and soot precursors.

Intermediate-species mole fractions in premixed flames of the four butanol isomers under identical conditions have not been reported to date. Examples are shown in Figure 22 for

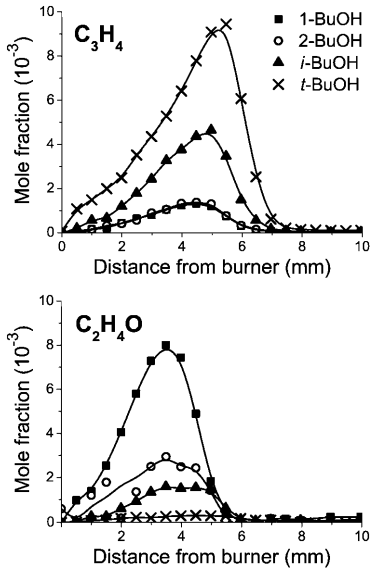

Figure 22. Mole-fraction profiles of C_3H_4 (sum of allene (CH_2CCH_2) and propyne (CH_3CCH)) and C_2H_4O (sum of CH_2CHOH and CH_3CHO) as a function of distance from burner, determined by EI-MBMS for fuel-rich ($\Phi = 1.71$) flames of the four butanol isomers.

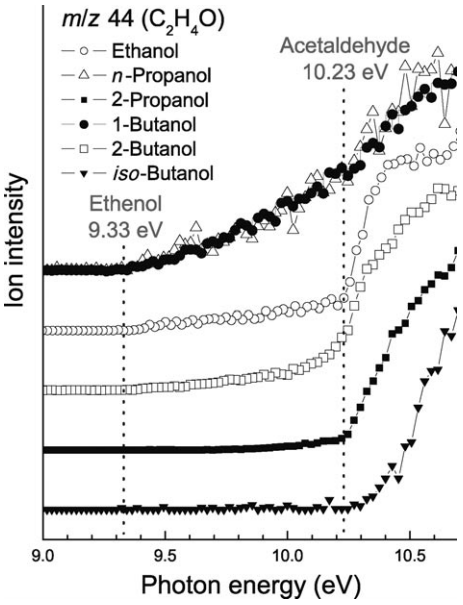

Figure 23. PIE spectra for m/z 44 species (C_2H_4O) sampled from the pyrolysis of alcohols. Dashed lines indicate the thresholds for ethenol (9.33 eV) and acetaldehyde (10.23 eV).

C_3H_4 (allene and propyne), representative of hydrocarbons and C_2H_4O (ethenol and acetyldehyde), representative of common oxygenated intermediates. The sums of the respective isomers were detected by EI-MBMS and were found to be in excellent agreement with independent PI-MBMS measurements (not shown), where isomers were separated. The results can be interpreted in light of the molecular structure and respective decomposition paths of the fuel. High C_3H_4 mole fractions in *tert*-butanol and *iso*-butanol flames arise from unimolecular H_2O elimination to form *iso*-butene and subsequently C_3H_4.[91] In contrast, the highest mole fractions for C_2H_4O are observed in 1-butanol and 2-butanol flames where direct reaction channels are available. Owing to the H_2O elimination reaction, oxygenate concentrations are lowest in *tert*-butanol flames. This reaction is an important variation from the common theme in alcohol combustion of preserving the C–O bond.

The presence of ethenol and its tautomeric counterpart acetaldehyde is now seen to be a general motif in alcohol pyrolysis.[17a,18] PIE spectra in Figure 23 indicate that the formation of C_2H_4O isomers has a distinct relationship with the structure of the alcohols, especially with the position of OH groups in the molecule. The importance of enols in combustion is generally being discussed,[92] also with respect to butanol oxidation.[92b] Reactions leading to their formation are still under intense study, but the authors of Ref. [92b] conclude that enols may be almost as abundant in flames as aldehydes.

The combustion chemistry of higher alcohols exhibits an even greater wealth of reactions than for hydrocarbon fuels. As details of the elementary kinetics and reaction mechanisms are becoming available, the eminent influence of the fuel structure on the intermediate-species pool cannot be denied. The nature and amounts of specific oxygenated compounds including undesired combustion emissions, such as aldehydes, ketones, and epoxides, are hard to predict without an in-depth understanding of the reaction sequences. In parallel to these detailed combustion studies, metabolic engineering explores routes to a variety of alcohols (Figure 24).[93] A critical evaluation of optimal strategies combining fuel synthesis and combustion performance will need intense collaboration across disciplines.

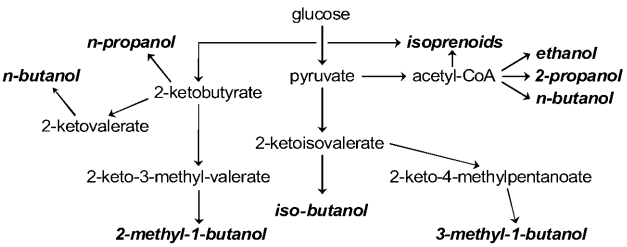

Figure 24. Schematic representation of engineered metabolic pathways to produce candidate biofuels. The biofuels described in the original article are given in italics. Reprinted from Ref. [93], copyright (2008), with permission from Elsevier.

4.6. Biodiesel: Esters

Rudolf Diesel's engine is reported to have run on peanut oil when demonstrated at the world exhibition in Paris in 1900, but direct use of vegetable oils presents problems of coking, low viscosity, and poor ignition.[25] Today's biodiesel fuels are methyl and ethyl esters of fatty acids from plant and animal provenance.[25,26,28] In different regions of the world, biodiesel can be produced from local crops, such as soy beans, rapeseed, palms, olives, sunflowers, or jatropha. Biodiesel can be blended with petroleum diesel or used as a neat fuel in current automotive engines, taking advantage of its low sulfur and aromatics content and of the substantial decrease in CO,

unburned hydrocarbons, and particulates in the exhaust gases.[25,26] However, NO_x, aldehyde, and ketone emissions may increase.[28] While petroleum diesel contains mainly saturated unbranched C_{12}–C_{18} hydrocarbons, practical biodiesel fuels present long carbon chains that may be branched and unsaturated. Because of the large size of these molecules and their chemical variability, the development of detailed combustion models is in its early stage.[94–98]

The combustion of rapeseed methyl ester, a blend of C_{14}–C_{22} esters, was studied in jet-stirred-reactor experiments and simulated with a kinetic model.[97] Reliable simulation for compounds such as methyl palmitate ($C_{17}H_{34}O_2$), methyl stearate ($C_{19}H_{38}O_2$), methyl oleate ($C_{19}H_{36}O_2$), methyl linoleate ($C_{19}H_{34}O_2$), and methyl linolenate ($C_{19}H_{32}O_2$), ingredients of rapeseed and soy-bean biodiesel, requires submodels that are being developed for simpler, but nevertheless challenging, examples, such as methyl butanoate,[96b,c,98,99] methyl butenoate,[96a] and methyl decanoate.[95,100] Several features of the combustion reactions for these esters are similar to those of large *n*-alkanes, such as *n*-hexadecane, because of the common alkyl chains.[97] Mechanisms tend to become complex, not only because of the size of the fuel molecules, but also as a consequence of the additional reactions of oxygen-containing species. For example, low-temperature ignition of methyl decanoate was modeled with 3012 species and 8820 reactions.[95] Important pathways for ester combustion include alkyl peroxy radical reactions, isomerization reactions, and H-atom transfer.[99]

Several aspects of ester oxidation cannot be reproduced by alkane models, however, including an early formation of CO_2 that was detected in jet-stirred-reactor experiments.[97] The origin of the observed CO_2 is linked to the fate of the two oxygen atoms in the molecule. Methyl esters can decompose into two separate reactive oxygen carriers which could contribute to soot-precursor reduction, or the O-C-O structure in the molecule may form CO_2. Both mechanisms have been discussed. To resolve this question by direct analysis, time histories for CO_2 formation have been measured in shock tubes by infrared laser absorption.[101] They confirm the high CO_2 yield found in flame[102] and reactor[96b] experiments. A reaction-flux analysis reveals the importance of the CH_3OCO intermediate that subsequently decomposes to CH_3 and CO_2. The prediction of correct CO_2 mole fractions has been a critical parameter in the development and improvement of the methyl butanoate mechanism used in this study, and modeling results are in quite good agreement with the measurements (Figure 25).[101]

Detailed kinetic mechanisms for ester combustion are important to understand the autoignition properties of biodiesel components in diesel engines, in particular because no octane ratings are available.[103] Autoignition of linear methyl esters from butanoic to octanoic acids was studied in rapid-compression-machine experiments and compared to that of related alkanes and alkenes.[103] Figure 26 shows that ignition timing is quite different even for a homologous series of methyl esters, with methyl butanoate being the most resistant fuel to autoignition. It is discussed that the reactivity increases with the length of the alkane chain. High reactivity is attributed to the methoxy radical. The detailed analysis of

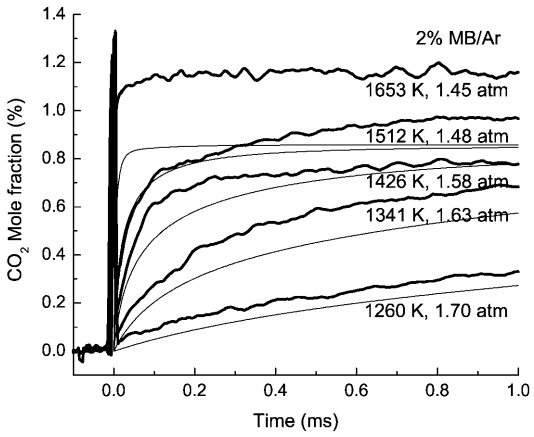

Figure 25. Calculated (thin lines) and measured (thick lines) CO_2 concentration time histories for methyl butanoate (MB) pyrolysis (2% MB in Ar). The CO_2 profiles were calculated using the improved MB model reported in Ref. [101]. Reprinted from Ref. [101], with permission from The Combustion Institute.

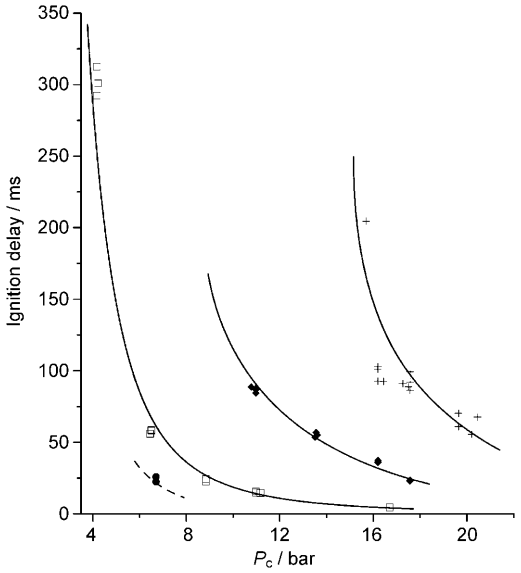

Figure 26. Autoignition delay times of fatty acid methyl esters around 815 ± 20 K, at high pressures, studied in a rapid compression machine. Gas mixtures are stoichiometric with "air" (nitrogen is replaced by argon). Methyl butanoate (+), methyl pentanoate (◆), methyl hexanoate (□), and methyl heptanoate (●). Reprinted from Ref. [103], with permission from The Combustion Institute.

the cool-flame region emphasizes the importance of H-atom transfer reactions which depend on the fuel structure. Reactions that may form a six-membered transition state are kinetically favored.[103] More generally, alkyl and alkyl ester radicals add to O_2 to form RO_2 radicals in the low-temperature regime, and they decompose in the high-temperature regime to form olefins and unsaturated esters which may then react further in similar elementary reactions.[100]

The combustion reactions of ethyl esters show mechanistic differences from those of methyl esters.[104,105] To emphasize structural effects, Oßwald et al.[102] have studied identical, rich premixed flames of the two smallest isomeric ester

prototypes for biodiesel combustion, ethyl formate and methyl acetate. While global combustion features such as temperature and major-species mole fractions are almost indistinguishable, intermediate species differ distinctly for the two fuels. The formation of most species and their respective mole fractions could be explained with acylic or alkylic H-abstraction and β-scission reactions. Mole fractions for C_2- to C_6-hydrocarbons are higher in the ethyl formate flame as a consequence of the ethyl group and carbon build-up reactions. However, they are still lower than those seen in comparable fuel-rich hydrocarbon flames, confirming a tendency of ester fuels to reduce soot precursors. With respect to oxygenated intermediates, H-abstraction from the methoxy group of the methyl ester leads preferentially to formaldehyde, and H-abstraction from the ethoxy group of the ethyl ester leads to greater mole fractions of acetaldehyde.[102]

These experiments were complemented with similarly detailed investigations for methyl formate and ethyl acetate flames to cover the complete range of structural variation.[94] All the flames were burned under comparable conditions, a considerable number of species was detected quantitatively with PI-MBMS, and the results were compared with simulations. Figure 27 summarizes some of the key observations. The kinetic model takes unimolecular decomposition and H-abstraction initiation reactions into account. For the methyl esters, the unimolecular decomposition will break a C–O bond to form CH_3 or CH_3O radicals. Ethyl esters can decompose through a unimolecular elimination reaction producing C_2H_4 via a six-membered pericyclic transition state. This ethene elimination reaction may be the reason why ethyl esters may ignite more rapidly.[105] Most species profiles depicted in Figure 27 are reasonably well reproduced with the kinetic model. C_2 species are more abundant in the ethyl ester flames because ethene can be produced directly from the ethyl groups (Figure 27, column a). Methyl ester flames produce more formaldehyde, a direct scission product (Figure 27, column b). H-abstraction and β-scission from the acetate group yields higher ketene mole fractions (Figure 27, column c), and methane is produced predominantly from methyl radicals (Figure 27, column d). Most acetaldehyde is found in the ethyl acetate flame, where it may be formed directly.[94]

To build on this database and extend it to larger ester fuels, we have started within our collaborative work to investigate the influence of important structural motifs on the combustion chemistry of esters. As one subset, flames of the C_5 isomers methyl butanoate, methyl isobutanoate, and ethyl propanoate have been studied by PI-MBMS under identical conditions.[106] Identification of intermediates relied on PIE curves, such as those shown in Figure 28. The three $C_5H_{10}O_2$ esters feature different intermediates, which can again be rationalized from an understanding of primary fuel-decomposition and oxidation reactions. The presence of several important oxygenated intermediates is observed with C_2H_2O at m/z 42 (ketene), C_3H_4O at m/z 56 (methyl ketene), and C_4H_6O at m/z 70 (ethyl ketene/dimethyl ketene). The subtle differences seen when comparing the three fuels are understandable from their decomposition mechanisms. For example, dimethyl ketene was identified in the methyl isobutanoate flame, and ethyl ketene was seen in the methyl butanoate flame. The formation of both can be understood

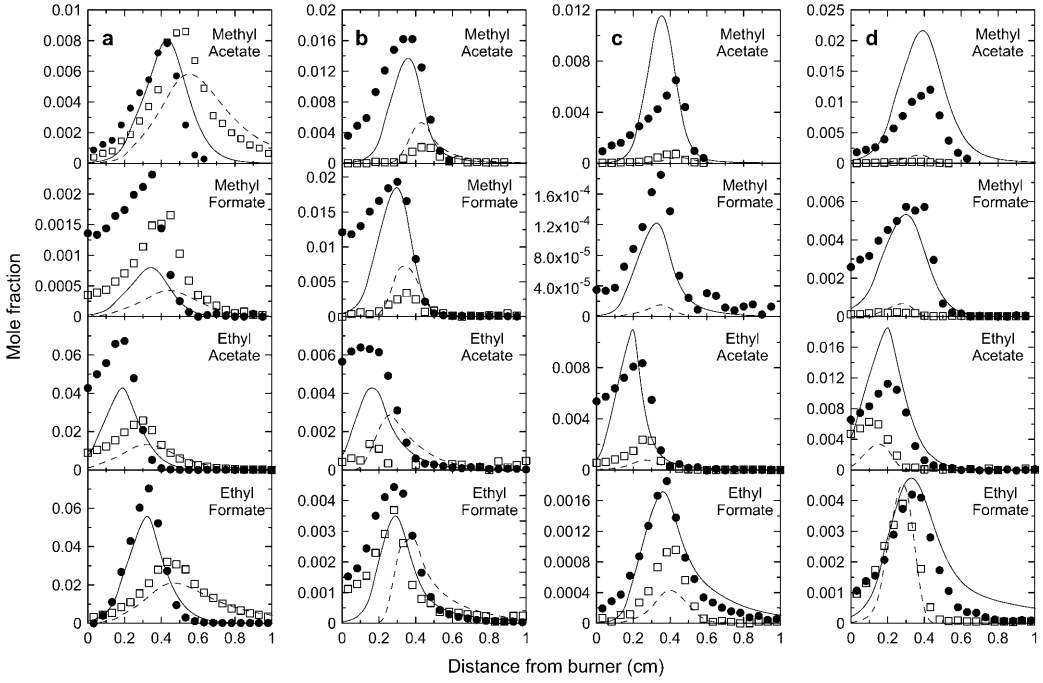

Figure 27. Experimental species profiles (symbols) compared with computed results (lines) for premixed (40 mbar) methyl acetate, methyl formate, ethyl acetate, and ethyl formate flames; dashed lines correlate with the open symbols, solid lines with the closed symbols. a) ethene (circles) and acetylene (squares); b) formaldehyde (circles) and formyl (squares; the values have been increased by a factor of 10 for clarity); c) ketene (circles) and propyne (squares; values have been increased by a factor of 10 for clarity); d) methane (circles) and acetaldehyde (squares). Reprinted from Ref. [94], with permission from The Combustion Institute.

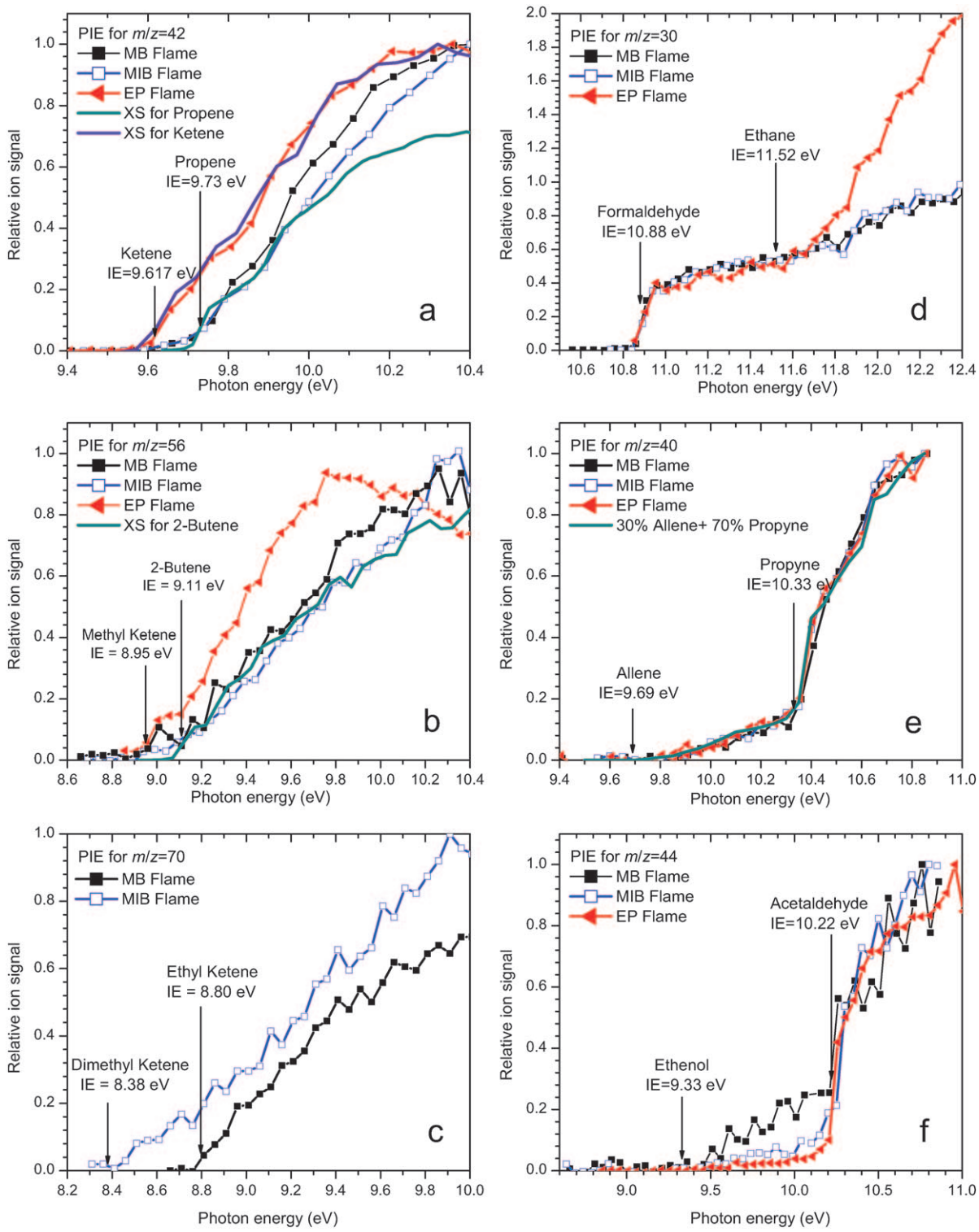

Figure 28. PIE spectra for selected intermediates in three premixed ester flames;[106] $\Phi = 1.56$, $p = 40$ mbar. MB: methyl butanoate, MIB: methyl isobutanoate, EP: ethyl propanoate.

from specific reaction sequences, analyzed in the original paper.[106] These species are not formed in the ethyl propanoate flame, where the respective pathways are not available. For the ethyl propanoate flame, characteristic features include the presence of ketene, methyl ketene, and of ethane (Figure 28). The decomposition reactions of ethyl propanoate are given in Figure 29 which highlights the plausible formation of some of the species in Figure 28.

As seen from Figure 26, the lower reactivity of these smaller fuel molecules is not representative for realistic biodiesel compounds. Also, many compounds in biodiesel are unsaturated esters, which may be less reactive towards low-

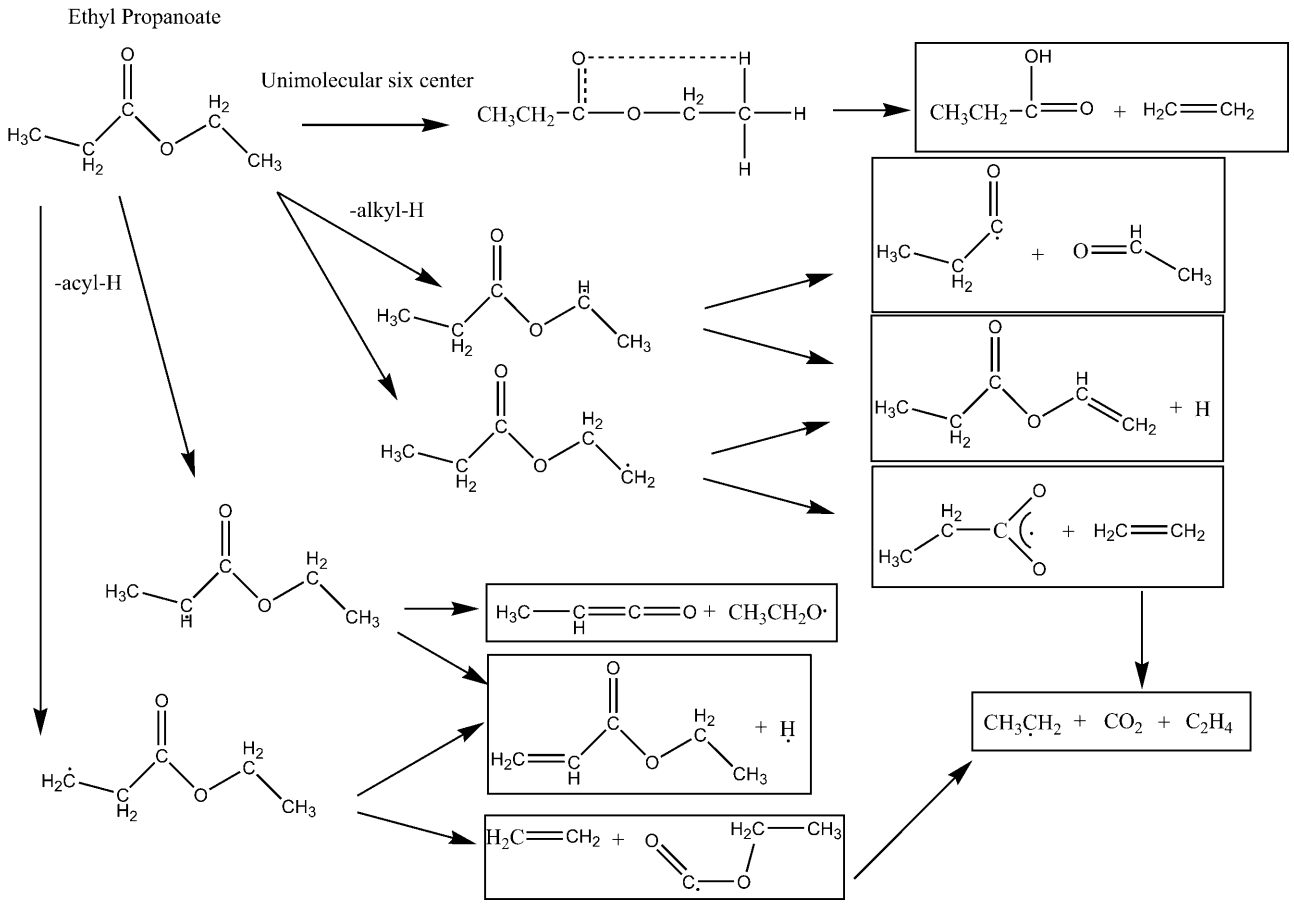

Figure 29. Pathways for the destruction of ethyl propanoate by unimolecular six-centered dissociation and H-atom abstraction from the alkyl and acyl function groups.[106]

temperature oxidation than the respective saturated molecules.[107] Furthermore, biodiesel typically contains more than one kind of ester. The combustion behavior and models for the smaller ester molecules above are thus not necessarily of direct practical relevance. However, combustion models for these smaller esters are important subsets for larger ones. Since the principal nature of the reaction steps that may occur is quite well understood, models for esters with longer chains—more realistic biodiesel compounds—are being developed following the experience with the detailed investigations on smaller prototypes.

Figure 30 presents details of the reaction flux for a biodiesel surrogate fuel consisting of methyl decanoate and methyl decenoate, illustrating the complexity of low-temperature oxidation of biodiesel fuels such as would occur in a diesel engine with biodiesel as the fuel.[108] This mechanism has been extended from that of Herbinet et al.[95] to include the chemistry related to the C=C bonds. The fuel radical-decomposition reaction pathways depend strongly on temperature. For the high-temperature regime, important reactions include unimolecular decomposition, reactions with small radicals which can be involved in H-abstraction and addition to the double bonds as well as isomerization steps, including cyclic transition states. At lower temperatures where ignition occurs, principal reactions include radical addition to O_2 and isomerization of the resulting RO_2 species. The model predicts early CO_2 formation and involves many reactions that are also seen in the low-temperature oxidation of hydocarbons.[109] Figure 30 shows the fate of the radical that is obtained from methyl decanoate upon abstraction of a secondary H-atom by OH radicals. At low temperature (Figure 30a, 650 K), an ROO radical is formed that isomerizes to three different further radicals of QOOH structure. The further steps in the oxidation involve ketohydroperoxides and four- and five-membered cyclic ethers. At higher combustion temperature (Figure 30b, 900 K), isomerization is seen to further C_{11} alkyl ester radicals. The reaction scheme also involves unsaturated compounds. Regarding decenoate oxidation, the double bond inhibits certain H-atom-transfer isomerization reactions. The presence and position of a double bond thus has an important influence on the low-temperature reactivity of the ester molecule.[108]

While biodiesel is being established on the market, the structural richness of biodiesel components gives combustion chemists a hard time. Mechanisms to describe the combustion chemistry of biodiesels in detail are developed in parallel to the use of these fuels on the road. In comparison to the alcohols discussed above, the absolute concentration and nature of emissions may be harder to predict. Even global properties, such as ignition timing, may have to be assessed individually for new compositions of esters in biodiesel fuels that may emerge when local oils or energy plants are used.

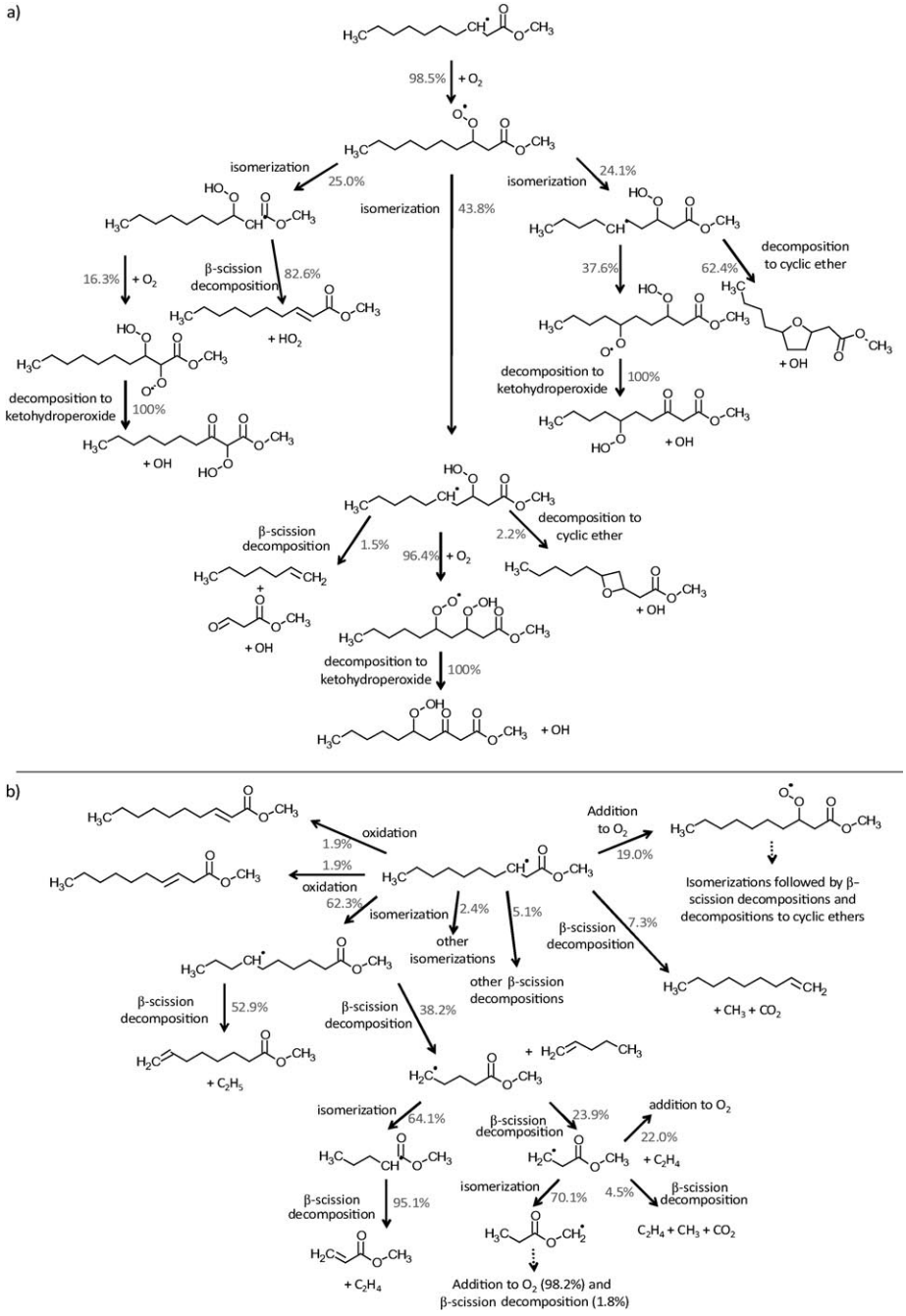

Figure 30. Flow decomposition paths of a radical formed by abstraction of a secondary H-atom from methyl decanoate at a residence time of 1 s and a temperature of a) 650 K and b) 900 K. Reprinted from Ref. [108], with permission from The Combustian Institute.

5. Perspectives: Nitrogen-Containing Biofuel Prototypes

Similarly to coal, almost all solid fuels from biomass or waste contain organically bound nitrogen. This is a significant source for the emission of NO_x from combustion processes. NO_x is a short form representing oxides of nitrogen including NO, NO_2, and N_2O. These undesirable combustion products are involved in photochemical smog, acid rain, and tropospheric ozone formation, N_2O is also an efficient greenhouse gas. While NO_x is also produced in conventional fossil-fuel combustion with air, it must be acknowledged that NO_x formation is the result of different chemical mechanisms.[110,111] "Thermal" NO is a product of radical reactions involving O- and N-atoms at high temperature. "Prompt" NO is formed in fuel-rich zones involving reactions of N species with CH radicals. A third mechanism involves conversion of fuel-bound nitrogen. With combustion strategies that avoid high-temperature peaks and include advanced burner design and fuel staging, the dominant source of NO_x in solid-fuel combustion is the oxidation of the fuel-bound nitrogen. In pulverized-coal combustion, fuel-nitrogen conversion to NO typically accounts for more than 80% of the NO emission.[110]

Table 3 shows that nitrogen contents in typical plant and waste matter are comparable with that of coal. The details of fuel-nitrogen conversion remain a topic of acute importance,[110,112–118] especially with respect to biomass and waste combustion. Volatile nitrogen-containing species released during gasification and pyrolysis of biomass include NH_3, HNCO, and HCN.[110,118] The schematic diagram in Figure 31 illustrates important reaction sequences for some nitrogenated compounds. In spite of the different starting substances and oxidation pathways, the final conversion of fuel nitrogen into N_2 or NO is almost independent of the specific fuel. This is reported to be a consequence of high combustion temperatures, in which the nitrogen atom is detached from the carbon it was bound to in the fuel molecule.[110] However, such similarities as in Figure 31 break down under very fuel-rich conditions or at lower temperatures,[110] and more detailed understanding of the specific mechanisms is needed.

Most of the knowledge on fuel-nitrogen conversion to date is based on coal combustion. The functional form in which nitrogen is bound depends on the specific fuel. For example, coal includes heterocyclic structures, while biomass has proteins as a major fuel-nitrogen source.[114,118] The amino acid composition varies seasonally and for plants from different climatic zones. NH_3 and HCN are released during biomass combustion as a function of many parameters, including the chemical structures present in the fuel, the heating rate and the residence time in the combustor.[113] No simple correlation can thus be given regarding nitrogen release, NH_3/HCN ratio, and NO_x emission. Mechanisms for HCN and ammonia oxidation are therefore subjects of intense study.[113,114,116,119,120] In a recent investigation of wood-bark pyrolysis, NH_3, HCN, and HNCO

Table 3: Typical nitrogen content in selected fuels.[110] RDF: refuse-derived fuel.

Fuel	N content [wt%]
Straw	0.3–1.5
Other agricultural residues	0.4–3.5
Wood	0.003-1.0
Peat	0.5–2.5
Coal	0.5–2.5
Paper	0.1–0.2
RDF	0.8
Tires	0.3
Household waste	0.5–1.0
Plastic waste	0.0
Sewage sludge	2.5–6.5

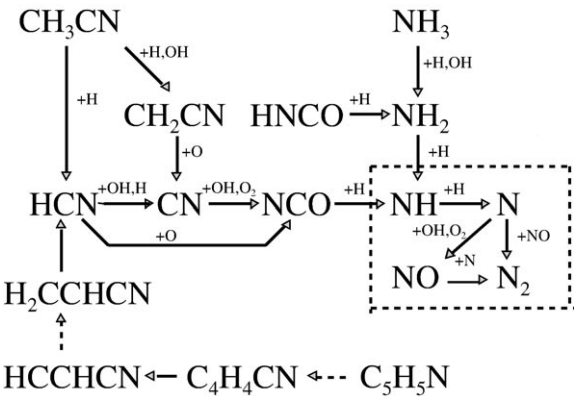

Figure 31. Reaction-path diagram illustrating major steps in volatile nitrogen conversion in flames for different nitrogen species (HCN, NH_3, HNCO, CH_3CN, and pyridine) at moderate fuel-nitrogen concentrations. Solid arrows denote elementary reaction pathways, dashed arrows denote routes that involve intermediates and reactions not shown. The diagram is based on modeling predictions with a detailed reaction mechanism based on the literature (see references in original article). Reprinted from Ref. [110], copyright Elsevier (2003), with permission from Elsevier.

were detected as nitrogen-containing volatiles.[118a] The ratio of NH_3 to HCN was very sensitive to temperature. Main products from protein nitrogen were NH_3, char nitrogen, and cyclic amides that formed HCN and HNCO as cracking products. The distribution of nitrogenous species in the pyrolysate did not depend primarily on the O/N ratio in the combustion process but rather on the nature of the of fuel nitrogen functional group.[118a] Similarly, the nitrogen inventory for gasification of coal and of biomass, including cane trash and sewage sludge,[114,118b] showed NH_3 and HCN as major volatile NO_x precursors and emphasized the role of char and tar nitrogen. Biomass pyrolysate was typically richer in NH_3 than that of coal, in which HCN is more dominant.[114,117]

Volatile and char-bound nitrogen are oxidized during biomass combustion and contribute to NO_x emissions. A novel mechanism has been described recently for the formation of NO in biomass combustion involving heterogeneously fixed nitrogen.[112] Experiments were performed with beech wood and with the pure biomass components cellulose, xylan (hemicellulose), and lignin, which are macromolecules from plant matter and have different structures. Pyrolysis was carried out in N_2 atmosphere at 900 °C and 1050 °C, and the resulting chars were oxidized by 10% O_2 in Ar at 700 °C; results are shown in Figure 32. Interestingly, the NO yield is

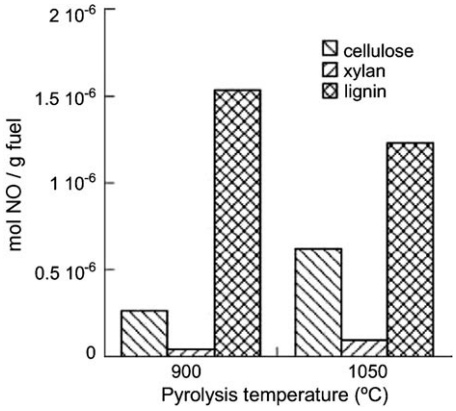

Figure 32. The NO emission from combustion of chars of cellulose, xylan (hemi-cellulose), and lignin, respectively. The chars were formed from pyrolysis in N_2 and subsequently oxidized in 10% O_2 in Ar at 700 °C. Reprinted from Ref. [112], with permission from The Combustion Institute.

different for these components of biomass, and it does not correlate directly with the nitrogen content of the respective char. Reasons for this difference are presently unclear. They may involve N_2 chemisorption on the char surface with cyano group formation during pyrolysis and subsequent NO release during oxidation.[112] Such interactions between volatile and char-fixed nitrogen increase the complexity of NO_x formation mechanisms from biomass and must be considered in detailed mechanisms.

Because of the importance of NH_3 as a NO_x precursor in biomass combustion, recent studies have addressed the detailed mechanisms of NH_3 oxidation in premixed low-pressure flames by using MBMS to identify intermediates.[119,120] Fuel blends of NH_3 with H_2[119] and CH_4[120] were investigated. The addition of H_2 can influence the concentration of NH_2 and NH radicals, which are important in fuel-nitrogen conversion (see Figure 31), and blends with CH_4 permit the study of realistic interactions of amine- and hydrocarbon-combustion chemistry. As an example, Figure 33 shows the concentrations of N_2O intermediates as a function of pressure. Even in this quite simple case of a H_2–NH_3–O_2–Ar flame, simulations with a flame model show deviations in the N_2O mole fractions that necessitate further study of the relevant kinetic parameters.[119] In the 11 flames of different NH_3–CH_4 blends, many species were identified, including C_2 hydrocarbons (such as C_2H_2, C_2H_4, and C_2H_6), oxygenates (such as CH_2O, CH_2CO, CH_3OH, CH_3CHO), and nitrogenated compounds (such as HCN, CH_2NH, NO, HCNO, HNCO, N_2O, CH_3NO, and NO_2).[120] Simulations of the experimental results were quite successful with a reaction mechanism involving 84 species and 703 reactions. From a sensitivity analysis, intermediates of key importance include CH_3, CH_2, NH_2, and NH radicals, as well as CH_2O and HNO.[120]

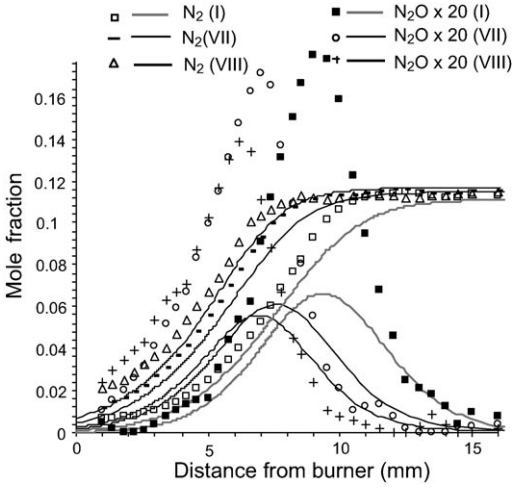

Figure 33. Comparison of the simulated (line) and experimental (symbols) mole-fraction profiles of N_2 and N_2O in a low-pressure premixed H_2–NH_3–O_2–Ar flame ($\Phi = 1.0$) according to the pressure (flame I: $p = 60$ mbar; VII: $p = 90$ mbar; VIII: $p = 120$ mbar). Reprinted from Ref. [119], with permission from The Combustion Institute.

While H,C,N,O intermediates are detected in these NH_3–CH_4 flames, the fuel does not have a carbon–nitrogen bond. Lucassen et al.[121] have recently studied the detailed combustion chemistry in a morpholine flame at low pressure by using EI- and PI-MBMS. Morpholine (1-oxa-4-aza-cyclohexane) is a cyclic ether and secondary amine. This heterocyclic compound is used as a fungicide, as an impregnating agent for fruit, cardboard, and paper, and as a fuel additive. The molecule bears structural resemblances to ethanol, dimethyl ether, ethyl amine, and dimethyl amine. The wealth of components detected with up to six heavy atoms presents a challenge regarding species identification. Pathways for initial decomposition were suggested including H-abstraction and ring-opening β-scission as well as homolytic cleavage reactions. These processes can explain the formation of most detected intermediates. With respect to undesired emissions, Figure 34 presents mole-fraction profiles for NO, CH_2O, NH_3, HCN, and HNCO. Only formaldehyde is seen to present a

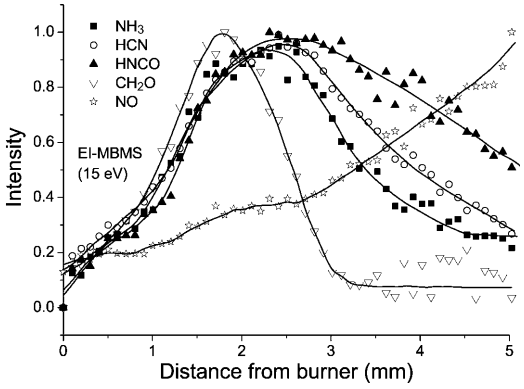

Figure 34. Species profiles for NO, CH_2O, NH_3, HCN, and HNCO from a premixed morpholine flame (40 mbar; $\Phi = 1.3$). Adapted from Ref. [121], with permission from The Combustion Institute.

typical intermediate-species profile, while those for NH_3, HCN, HNCO, and especially NO persist well into the burnt-gas region.[121] Interesting aspects in these flames of nitrogenated fuels include the detection of the tautomeric pair of ethenamine and acetaldimine. Also, a species of composition C_2H_3N is detected that could be 2*H*-azirine.[121,122] It will be interesting in fuel–air flames of nitrogenated fuels to separate the contributions to NO_x formation from fuel-bound nitrogen conversion and from the prompt mechanism, because CH radicals are also formed and can interact with the nitrogenated species. Laser-diagnostic measurements of small intermediates of key importance which include NH_2, CN, CH, and NCN can assist in resolving these mechanistic details.

Recent investigations with isomer-resolving PI-MBMS include flames of aromatic heterocycles, such as pyrrole[122] and pyridine,[123] small molecules that are representative of such structures in coal and other low-rank fuel combustion. The full range of combustion intermediates with $m/z < 160$ had not been detected and identified until very recently, owing to the richness of compounds with different structures present in these flames. Figure 35 shows a reaction-path

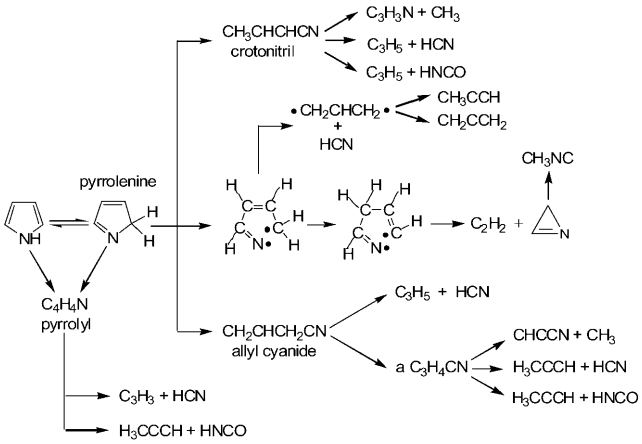

Figure 35. Reaction-path diagram illustrating the oxidation process of pyrrole in low-pressure (33 mbar) premixed flames. Reprinted from Ref. [122], with permission from The Combustion Institute.

diagram for pyrrole combustion.[122] N_2, NO, and NO_2 are the main nitrogenated products, and HCN, HNCO, and 2-propenenitrile (CH_2CHCN) are the most abundant nitrogen-containing intermediates. Typical hydrocarbon species from the C_1 to C_5 families are detected, as well as many further nitrogenated compounds.[122] The analysis of the oxidation pathways for these and other nitrogen-containing fuels awaits the availability of detailed combustion models.

Pollutant formation from biomass fuels is a complex problem which involves reactions of volatile compounds as well as heterogeneous reactions. Chemically, these fuels are not well-defined and present a broad bandwidth of structural elements. Furthermore, additional elements must be considered, such as sulfur[124] and chlorine.[125] Compared to alcohol, ether, and ester biofuels, detailed chemical pathways for the combustion of prototypical biomass compounds are even more complex and only just emerging.

6. Conclusions

Biofuels are present on the market in different countries, and their share is increasing. The perceived problem in the public discussion is their competition with food plants. Also, economic and climatic factors are considered at least partially unresolved. Technical aspects of concern include the consequences for the delivery infrastructure and the adaptation to present combustion systems. Furthermore, intense research is devoted to low-energy, low-cost techniques to make such fuels using chemical or biotechnological strategies. Herein we have reviewed the combustion chemistry of some current biofuel compounds. One of the most important messages is that "biofuel" is a chemically very heterogeneous and variable term. Typical members of biofuel families including alcohols, ethers, esters, and some nitrogenated chemicals have been discussed with particular emphasis on harmful combustion emissions. A most general conclusion is that the innate chemical structure of the fuel molecule always matters with respect to the intermediates and products formed, including pollutants.

Intimate knowledge of the chemical reaction network involved is a prerequisite to determine the value of a biofuel with respect to combustion emissions. Typical biofuels can produce PAHs and soot, similar to conventional hydrocarbon fuels. These emissions may be reduced with respect to pure hydrocarbon molecules of similar size. Often, this benefit is paid for with increased formation of carbonyl compounds, including formaldehyde, acetaldehyde, acetone, and higher aldehydes and ketones. Larger molecules may present more variation in the spectrum of intermediates; for example, butanols may form higher-mass oxygenates than ethanol. Because isomeric variants of fuels such as butanol and biodiesel give rise to different sequences of elementary reactions, the intermediate and product spectrum differ as well. Additional chemical functions in the biofuel molecule, such as the presence of nitrogen in amines and heterocycles, open avenues to additional species and toxic emissions. Unspecified plant and waste matter as a basis for biomass fuels may involve further elements from the periodic table. While phenomenological combustion behavior of such fuels with respect to changes in temperature, pressure, stoichiometry, and residence time may be available, predictive combustion modeling to assess the emission potential will emerge more slowly for more challenging fuel compounds and fuel mixtures. The chemically simpler compounds such as small alcohols and ethers are more easily judged in this respect than the more complex biodiesel and wood pyrolysate ingredients. Mixtures of conventional fossil fuels with biofuels, such as petroleum diesel with biodiesel, may open up further chemical pathways through the interaction of the decomposition and oxidation of all the components in the mixture. It may thus be wiser to judge a biofuel beyond its economic viability or technical ease of adaptation to the present combustion environment.

The authors wish to thank the numerous present and past students and postdocs in their groups who have been instrumental in the research highlighted in this Review. Many of them are named as co-authors in the original articles cited in this work. In particular, Hanna Güldenberg, Nicole Labbe, Wenjun Li, Yuyang Li, Zhenyu Tian, Jing Wang, and Bin Yang are acknowledged for their valuable contributions to the data collection and evaluation for many of the experiments covered herein. K.K.H. is grateful to Michael Letzgus and Kuiwen Zhang for the design of the title graphics and to Regine Schröder for assisting with some technical details in the preparation of the manuscript. Also, K.K.H. acknowledges continuing support of part of this research by DFG under contracts KO1363/18-1 and 18-3, by Fonds der Chemischen Industrie, and by the German Academic Exchange Service. The work has also been supported by the Division of Chemical Sciences, Office of Basic Energy Sciences, US Department of Energy (USDOE), in part under grants DE-FG02-01ER15180 (T.A.C.) and DE-FG02-91ER14192 (P.R.W.), and by the Chemical Sciences Division, US Army Research Office (T.A.C.). Sandia is a multi-program laboratory operated by Sandia Corporation, a Lockheed Martin Company, for the National Nuclear Security Administration under contract DE-AC04-94-AL85000. The Advanced Light Source is supported by the Director, Office of Science, Office of Basic Energy Sciences, Materials Sciences Division of the USDOE under contract DE-AC02-05CH11231 at Lawrence Berkeley Laboratory. F.Q. is grateful for support of part of this research by the Chinese Academy of Sciences (CAS), Natural Science Foundation of China under grant 50925623, National Basic Research Program of China (973) under grant 2007CB815204, and Ministry of Science and Technology of China under grant 2007DFA61310. Finally, K.K.H. expresses her gratitude to Jason Hill, Mani Sarathy, Priyank Saxena, Philippe Dagaut, Thomas Litzinger, Charles McEnally, James Liao, David Davidson, Rodolphe Minetti, Peter Glarborg, and Catherine Duynslaegher for providing original graphics for Figures 1, 2, 5, 11, 12, 13, 24, 25, 26, 31–33.

Received: September 23, 2009

[1] J. Fargione, J. Hill, D. Tilman, S. Polasky, P. Hawthorne, *Science* **2008**, *319*, 1235 – 1238.
[2] Ö. Gustafsson, M. Kruså, Z. Zencak, R. J. Sheesley, L. Granat, E. Engström, P. S. Praveen, P. S. P. Rao, C. Leck, H. Rodhe, *Science* **2009**, *323*, 495 – 498.
[3] L. Jaeglé, L. Steinberger, R. V. Martin, K. Chance, *Faraday Discuss.* **2005**, *130*, 407 – 423.
[4] P. J. Crutzen, A. R. Mosier, K. A. Smith, W. Winiwarter, *Atmos. Chem. Phys.* **2008**, *8*, 389 – 395.
[5] T. Searchinger, R. Heimlich, R. A. Houghton, F. Dong, A. Elobeid, J. Fabiosa, S. Tokgoz, D. Hayes, T.-H. Yu, *Science* **2008**, *319*, 1238 – 1240.
[6] D. Tilman, R. Socolow, J. A. Foley, J. Hill, E. Larson, L. Lynd, S. Pacala, J. Reilly, T. Searchinger, C. Somerville, R. Williams, *Science* **2009**, *325*, 270 – 271.
[7] D. Tilman, J. Hill, C. Lehman, *Science* **2006**, *314*, 1598 – 1600.
[8] a) L. D. Schmidt, P. J. Dauenhauer, *Nature* **2007**, *447*, 914 – 915; b) M. Stöcker, *Angew. Chem.* **2008**, *120*, 9340 – 9351; *Angew. Chem. Int. Ed.* **2008**, *47*, 9200 – 9211; c) J. O. Metzger, *Angew. Chem.* **2006**, *118*, 710 – 713; *Angew. Chem. Int. Ed.* **2006**, *45*, 696 – 698; *Angew. Chem.* **2006**, *118*, 710 – 713.
[9] G. Stephanopoulos, *Science* **2007**, *315*, 801 – 804.
[10] S. Atsumi, T. Hanai, J. C. Liao, *Nature* **2008**, *451*, 86 – 90.

[11] S. M. Sarathy, M. J. Thomson, C. Togbé, P. Dagaut, F. Halter, C. Mounaïm-Rouselle, *Combust. Flame* **2009**, *156*, 852 – 864.
[12] J. A. Miller, J. Troe, M. J. Pilling, *Proc. Combust. Inst.* **2005**, *30*, 43 – 88.
[13] J. Buckmaster, P. Clavin, A. Liñán, M. Matalon, N. Peters, G. Sivashinsky, F. A. Williams, *Proc. Combust. Inst.* **2005**, *30*, 1 – 19.
[14] C. K. Westbrook, Y. Mizobuchi, T. J. Poinsot, P. J. Smith, J. Warnatz, *Proc. Combust. Inst.* **2005**, *30*, 125 – 157.
[15] K. Kohse-Höinghaus, R. S. Barlow, M. Aldén, J. Wolfrum, *Proc. Combust. Inst.* **2005**, *30*, 89 – 123.
[16] C. S. McEnally, L. D. Pfefferle, B. Atakan, K. Kohse-Höinghaus, *Prog. Energy Combust. Sci.* **2006**, *32*, 247 – 294.
[17] a) T. A. Cool, K. Nakajima, T. A. Mostefaoui, F. Qi, A. McIlroy, P. R. Westmoreland, M. E. Law, L. Poisson, D. S. Peterka, M. Ahmed, *J. Chem. Phys.* **2003**, *119*, 8356 – 8365; b) N. Hansen, T. A. Cool, P. R. Westmoreland, K. Kohse-Höinghaus, *Prog. Energy Combust. Sci.* **2009**, *35*, 168 – 191; c) Y. Li, F. Qi, *Acc. Chem. Res.* **2010**, *43*, 68 – 78.
[18] C. A. Taatjes, N. Hansen, A. McIlroy, J. A. Miller, J. P. Senosiain, S. J. Klippenstein, F. Qi, L. Sheng, Y. Zhang, T. A. Cool, J. Wang, P. R. Westmoreland, M. E. Law, T. Kasper, K. Kohse-Höinghaus, *Science* **2005**, *308*, 1887 – 1889.
[19] C. A. Taatjes, N. Hansen, D. L. Osborn, K. Kohse-Höinghaus, T. A. Cool, P. R. Westmoreland, *Phys. Chem. Chem. Phys.* **2008**, *10*, 20 – 34.
[20] U. Struckmeier, P. Oßwald, T. Kasper, L. Böhling, M. Heusing, M. Köhler, A. Brockhinke, K. Kohse-Höinghaus, *Z. Phys. Chem.* **2009**, *223*, 503 – 537.
[21] J. Ballester, J. Barroso, L. M. Ceredo, R. Ichaso, *Combust. Flame* **2005**, *141*, 204 – 215.
[22] R. I. Backreedy, L. M. Fletcher, J. M. Jones, L. Ma, M. Pourkashanian, A. Williams, *Proc. Combust. Inst.* **2005**, *30*, 2955 – 2964.
[23] B. Damstedt, J. M. Pederson, D. Hansen, T. Knighton, J. Jones, C. Christensen, L. Baxter, D. Tree, *Proc. Combust. Inst.* **2007**, *31*, 2813 – 2820.
[24] a) A. Demirbas, *Prog. Energy Combust. Sci.* **2004**, *30*, 219 – 230; b) A. Demirbas, *Prog. Energy Combust. Sci.* **2005**, *31*, 171 – 192.
[25] A. K. Agarwal, *Prog. Energy Combust. Sci.* **2007**, *33*, 233 – 271.
[26] A. Demirbas, *Prog. Energy Combust. Sci.* **2007**, *33*, 1 – 18.
[27] H. Chen, S.-J. Shuai, J.-X. Wang, *Proc. Combust. Inst.* **2007**, *31*, 2981 – 2989.
[28] M. Lapuerta, O. Armas, J. Rodríguez-Fernández, *Prog. Energy Combust. Sci.* **2008**, *34*, 198 – 223.
[29] S. Adachi, A. Iwamoto, S. Hayashi, H. Yamada, S. Kaneko, *Proc. Combust. Inst.* **2007**, *31*, 3131 – 3138.
[30] C. D. Bolzso, V. G. McDonell, *Proc. Combust. Inst.* **2009**, *32*, 2949 – 2956.
[31] T. Fang, C. F. Lee, *Proc. Combust. Inst.* **2009**, *32*, 2785 – 2792.
[32] J. M. Anderlohr, A. Piperel, A. Pires da Cruz, R. Bounaceur, F. Battin-Leclerc, P. Dagaut, X. Montagne, *Proc. Combust. Inst.* **2009**, *32*, 2851 – 2859.
[33] R. J. H. Klein-Douwel, A. J. Donkerbroek, A. P. van Vliet, M. D. Boot, L. M. T. Somers, R. S. G. Baert, N. J. Dam, J. J. ter Meulen, *Proc. Combust. Inst.* **2009**, *32*, 2817 – 2825.
[34] U.S. Department of Energy, Alternative Fuels and Advanced Vehicles Data Center, http://www.afdc.energy.gov/afdc/ethanol/production.html, Download of Aug. 29, 2009.
[35] M. Balat, H. Balat, C. Öz, *Prog. Energy Combust. Sci.* **2008**, *34*, 551 – 573.
[36] R. F. Service, *Science* **2007**, *315*, 1488 – 1491.
[37] T. S. Norton, F. L. Dryer, *Int. J. Chem. Kinet.* **1992**, *24*, 319 – 344.
[38] N. M. Marinov, *Int. J. Chem. Kinet.* **1999**, *31*, 183 – 220.
[39] P. Saxena, F. A. Williams, *Proc. Combust. Inst.* **2007**, *31*, 1149 – 1156.
[40] N. Leplat, A. Seydi, J. Vandooren, *Combust. Sci. Technol.* **2008**, *180*, 519 – 532.
[41] R. Seiser, S. Humer, K. Seshadri, E. Pucher, *Proc. Combust. Inst.* **2007**, *31*, 1173 – 1180.
[42] T. S. Kasper, P. Oßwald, M. Kamphus, K. Kohse-Höinghaus, *Combust. Flame* **2007**, *150*, 220 – 231.
[43] D. Cipolat, N. Bhana, *Fuel Process. Technol.* **2009**, *90*, 1107 – 1113.
[44] T. Lie, M. Suzuki, H. Ogawa, *Fuel* **2009**, *88*, 2017 – 2024.
[45] E. Weber de Menezes, R. da Silva, R. Cataluña, R. J. C. Ortega, *Fuel* **2006**, *85*, 815 – 822.
[46] L. Zhang, Z. Huang, *Energy* **2007**, *32*, 1896 – 1904.
[47] C. Huang, M. Yao, X. Lu, Z. Huang, *Int. J. Therm. Sci.* **2009**, *48*, 1814 – 1822.
[48] Y. L. Wang, A. T. Holley, C. Ji, F. N. Egolfopoulos, T. T. Tsotsis, H. J. Curran, *Proc. Combust. Inst.* **2009**, *32*, 1035 – 1042.
[49] Z. Zhao, A. Kazakov, F. L. Dryer, *Combust. Flame* **2004**, *139*, 52 – 60.
[50] X. Qin, Y. Ju, *Proc. Combust. Inst.* **2005**, *30*, 233 – 240.
[51] X. L. Zheng, T. F. Lu, C. K. Law, C. K. Westbrook, H. J. Curran, *Proc. Combust. Inst.* **2005**, *30*, 1101 – 1109.
[52] E. W. Kaiser, T. J. Wallington, M. D. Hurley, J. Platz, H. J. Curran, W. J. Pitz, C. K. Westbrook, *J. Phys. Chem. A* **2000**, *104*, 8194 – 8206.
[53] A. McIlroy, T. D. Hain, H. A. Michelsen, T. A. Cool, *Proc. Combust. Inst.* **2000**, *28*, 1647 – 1653.
[54] H. J. Curran, W. J. Pitz, C. K. Westbrook, P. Dagaut, J. C. Boettner, M. Cathonnet, *Int. J. Chem. Kinet.* **1998**, *30*, 229 – 241.
[55] a) S. L. Fischer, F. L. Dryer, H. J. Curran, *Int. J. Chem. Kinet.* **2000**, *32*, 713 – 740; b) H. J. Curran, S. L. Fischer, F. L. Dryer, *Int. J. Chem. Kinet.* **2000**, *32*, 741 – 759.
[56] Z. Zhao, M. Chaos, A. Kazakov, F. L. Dryer, *Int. J. Chem. Kinet.* **2008**, *40*, 1 – 18.
[57] T. A. Cool, J. Wang, N. Hansen, P. R. Westmoreland, F. L. Dryer, Z. Zhao, A. Kazakov, T. Kasper, K. Kohse-Höinghaus, *Proc. Combust. Inst.* **2007**, *31*, 285 – 293.
[58] J. Wang, M. Chaos, B. Yang, T. A. Cool, F. L. Dryer, T. Kasper, N. Hansen, P. Oßwald, K. Kohse-Höinghaus, P. R. Westmoreland, *Phys. Chem. Chem. Phys.* **2009**, *11*, 1328 – 1339.
[59] C. Yao, X. Yang, R. R. Raine, C. Cheng, Z. Tian, Y. Li, *Energy Fuels* **2009**, *23*, 3543 – 3548.
[60] T. Ogura, Y. Sakai, A. Miyoshi, M. Koshi, P. Dagaut, *Energy Fuels* **2007**, *21*, 3233 – 3239.
[61] J. H. Mack, D. L. Flowers, B. A. Buchholz, R. W. Dibble, *Proc. Combust. Inst.* **2005**, *30*, 2693 – 2700.
[62] X. Pang, Y. Mu, J. Yuan, H. He, *Atmos. Environ.* **2008**, *42*, 1349 – 1358.
[63] A. Piperel, P. Dagaut, X. Montagne, *Proc. Combust. Inst.* **2009**, *32*, 2861 – 2868.
[64] C. Renard, P. J. van Tiggelen, J. Vandooren, *Proc. Combust. Inst.* **2002**, *29*, 1277 – 1284.
[65] K. Hoon Song, P. Nag, T. A. Litzinger, D. C. Haworth, *Combust. Flame* **2003**, *135*, 341 – 349.
[66] C. S. McEnally, L. D. Pfefferle, *Proc. Combust. Inst.* **2007**, *31*, 603 – 610.
[67] K. Kohse-Höinghaus, P. Oßwald, U. Struckmeier, T. Kasper, N. Hansen, C. A. Taatjes, J. Wang, T. A. Cool, S. Gon, P. R. Westmoreland, *Proc. Combust. Inst.* **2007**, *31*, 1119 – 1127.
[68] J. Wang, U. Struckmeier, B. Yang, T. A. Cool, P. Oßwald, K. Kohse-Höinghaus, T. Kasper, N. Hansen, P. R. Westmoreland, *J. Phys. Chem. A* **2008**, *112*, 9255 – 9265.
[69] Z. Chen, X. Qin, Y. Ju, Z. Zhao, M. Chaos, F. L. Dryer, *Proc. Combust. Inst.* **2007**, *31*, 1215 – 1222.
[70] P. Dagaut, C. Togbé, *Fuel* **2010**, *89*, 280 – 286.
[71] B. A. Bennett, C. S. McEnally, L. D. Pfefferle, M. D. Smooke, M. B. Colket, *Combust. Flame* **2009**, *156*, 1289 – 1302.
[72] K. L. McNesby, A. W. Miziolek, T. Nguyen, F. C. Delucia, R. R. Skaggs, T. A. Litzinger, *Combust. Flame* **2005**, *142*, 413 – 427.

[73] R. D. Cook, D. F. Davidson, R. K. Hanson, *Proc. Combust. Inst.* **2009**, *32*, 189 – 196.
[74] J. Zádor, R. X. Fernandes, Y. Georgievskii, G. Meloni, C. A. Taatjes, J. A. Miller, *Proc. Combust. Inst.* **2009**, *32*, 271 – 277.
[75] a) M. T. Holtzapple, R. R. Davidson, M. K. Ross, S. Aldrett-Lee, M. Nagwani, C.-M. Lee, C. Lee, S. Adelson, W. Kaar, D. Gaskin, H. Shirage, N.-S. Chang, V. S. Chang, M. E. Loescher, *Appl. Biochem. Biotechnol. Part A* **1999**, *79*, 609 – 631; b) S. Atsumi, J. C. Liao, *Appl. Environ. Microbiol.* **2008**, *74*, 7802 – 7808; c) C. R. Shen, J. C. Liao, *Metab. Eng.* **2008**, *10*, 312 – 320.
[76] T. Kasper, P. Oßwald, U. Struckmeier, K. Kohse-Höinghaus, C. A. Taatjes, J. Wang, T. A. Cool, M. E. Law, A. Morel, P. R. Westmoreland, *Combust. Flame* **2009**, *156*, 1181 – 1201.
[77] A. Frassoldati, A. Cuoci, T. Faravelli, U. Niemann, E. Ranzi, R. Seiser, K. Seshadri, *Combust. Flame* **2010**, *157*, 2 – 16.
[78] Y. Li, L. Wei, Z. Tian, B. Yang, J. Wang, T. Zhang, F. Qi, *Combust. Flame* **2008**, *152*, 336 – 359.
[79] T. Kasper, U. Struckmeier, P. Oßwald, K. Kohse-Höinghaus, *Proc. Combust. Inst.* **2009**, *32*, 1285 – 1292.
[80] A. Sinha, M. J. Thomson, *Combust. Flame* **2004**, *136*, 548 – 556.
[81] E. Zervas, X. Montagne, J. Lahaye, *Environ. Sci. Technol.* **2002**, *36*, 2414 – 2421.
[82] a) T. Ezeji, N. Qureshi, H. P. Blaschek, *Process Biochem.* **2007**, *42*, 34 – 39; b) Y. Ni, Z. Sun, *Appl. Microbiol. Biotechnol.* **2009**, *83*, 415 – 423; c) P. Dürre, *Ann. N. Y. Acad. Sci.* **2008**, *1125*, 353 – 362.
[83] a) T. Kasper, N. Hansen, J. Wang, B. Yang, T. A. Cool, P. R. Westmoreland, *Western States of the Combustion Institute Fall Meeting* **2007**, Sandia National Laboratories, Livermore, CA, USA, Oct. 16 – 17, 2007, Paper 07F08; b) P. Dagaut, B. McGuiness, J. M. Simmie, M. Cathonnet, *Combust. Sci. Technol.* **1998**, *135*, 3 – 29.
[84] P. Dürre, *Biotechnol. J.* **2007**, *2*, 1525 – 1534.
[85] R. Gheshlaghi, J. M. Scharer, M. Moo-Young, C. P. Chou, *Biotechnol. Adv.* **2009**, *27*, 764 – 781.
[86] a) A. M. López-Contreras, P. A. M. Claassen, H. Mooibroek, W. M. De Vos, *Appl. Microbiol. Biotechnol.* **2000**, *54*, 162 – 167; b) N. Qureshi, X.-L. Li, S. Hughes, B. C. Saha, M. A. Cotta, *Biotechnol. Prog.* **2006**, *22*, 673 – 680; c) N. Qureshi, T. C. Ezeji, J. Ebener, B. S. Dien, M. A. Cotta, H. P. Blaschek, *Bioresour. Technol.* **2008**, *99*, 5915 – 5922.
[87] S. Atsumi, T.-Y. Wu, E. M. Eckl, S. D. Hawkins, T. Buelter, J. C. Liao, *Appl. Microbiol. Biotechnol.* **2010**, *85*, 651 – 657.
[88] C. S. McEnally, L. D. Pfefferle, *Proc. Combust. Inst.* **2005**, *30*, 1363 – 1370.
[89] B. Yang, P. Oßwald, Y. Li, J. Wang, L. Wei, Z. Tian, F. Qi, K. Kohse-Höinghaus, *Combust. Flame* **2007**, *148*, 198 – 209.
[90] P. Dagaut, S. M. Sarathy, M. J. Thomson, *Proc. Combust. Inst.* **2009**, *32*, 229 – 237.
[91] J. T. Moss, A. M. Berkowitz, M. A. Oehlschlaeger, J. Biet, V. Warth, P.-A. Glaude, F. Battin-Leclerc, *J. Phys. Chem. A* **2008**, *112*, 10843 – 10855.
[92] a) C. A. Taatjes, N. Hansen, J. A. Miller, T. A. Cool, J. Wang, P. R. Westmoreland, M. E. Law, T. Kasper, K. Kohse-Höinghaus, *J. Phys. Chem. A* **2006**, *110*, 3254 – 3260; b) J. M. Simmie, H. J. Curran, *J. Phys. Chem. A* **2009**, *113*, 7834 – 7845.
[93] S. Atsumi, J. C. Liao, *Curr. Opin. Biotechnol.* **2008**, *19*, 414 – 419.
[94] C. K. Westbrook, W. J. Pitz, P. R. Westmoreland, F. L. Dryer, M. Chaos, P. Osswald, K. Kohse-Höinghaus, T. A. Cool, J. Wang, B. Yang, N. Hansen, T. Kasper, *Proc. Combust. Inst.* **2009**, *32*, 221 – 228.
[95] O. Herbinet, W. J. Pitz, C. K. Westbrook, *Combust. Flame* **2008**, *154*, 507 – 528.
[96] a) S. Gaïl, S. M. Sarathy, M. J. Thomson, P. Diévart, P. Dagaut, *Combust. Flame* **2008**, *155*, 635 – 650; b) S. Gaïl, M. J. Thomson, S. M. Sarathy, S. A. Syed, P. Dagaut, P. Diévart, A. J. Marchese, F. L. Dryer, *Proc. Combust. Inst.* **2007**, *31*, 305 – 311; c) S. M. Sarathy, S. Gaïl, S. A. Syed, M. J. Thomson, P. Dagaut, *Proc. Combust. Inst.* **2007**, *31*, 1015 – 1022.
[97] P. Dagaut, S. Gaïl, M. Sahasrabudhe, *Proc. Combust. Inst.* **2007**, *31*, 2955 – 2961.
[98] S. Dooley, H. J. Curran, J. M. Simmie, *Combust. Flame* **2008**, *153*, 2 – 32.
[99] C. J. Hayes, D. R. Burgess, Jr., *Proc. Combust. Inst.* **2009**, *32*, 263 – 270.
[100] K. Seshadri, T. Lu, O. Herbinet, S. Humer, U. Niemann, W. J. Pitz, R. Seiser, C. K. Law, *Proc. Combust. Inst.* **2009**, *32*, 1067 – 1074.
[101] A. Farooq, D. F. Davidson, R. K. Hanson, L. K. Huynh, A. Violi, *Proc. Combust. Inst.* **2009**, *32*, 247 – 253.
[102] P. Osswald, U. Struckmeier, T. Kasper, K. Kohse-Höinghaus, J. Wang, T. A. Cool, N. Hansen, P. R. Westmoreland, *J. Phys. Chem. A* **2007**, *111*, 4093 – 4101.
[103] K. HadjAli, M. Crochet, G. Vanhove, M. Ribaucour, R. Minetti, *Proc. Combust. Inst.* **2009**, *32*, 239 – 246.
[104] S. M. Walton, M. S. Wooldridge, C. K. Westbrook, *Proc. Combust. Inst.* **2009**, *32*, 255 – 262.
[105] W. K. Metcalfe, C. Togbé, P. Dagaut, H. J. Curran, J. M. Simmie, *Combust. Flame* **2009**, *156*, 250 – 260.
[106] B. Yang, J. Wang, T. A. Cool, T. Kasper, N. Hansen, K. Kohse-Höinghaus, *Proc. Sixth U.S. National Combustion Meeting* **2009**, Ann Arbor, Michigan, USA, May 17 – 20, 2009, Paper 22H3.
[107] Y. Zhang, Y. Yang, A. L. Boehman, *Combust. Flame* **2009**, *156*, 1202 – 1213.
[108] O. Herbinet, W. J. Pitz, C. K. Westbrook, *Combust. Flame* **2010**, *157*, 893 – 908.
[109] F. Battin-Leclerc, *Prog. Energy Combust. Sci.* **2008**, *34*, 440 – 498.
[110] P. Glarborg, A. D. Jensen, J. E. Johnsson, *Prog. Energy Combust. Sci.* **2003**, *29*, 89 – 113.
[111] J. A. Miller, C. T. Bowman, *Prog. Energy Combust. Sci.* **1989**, *15*, 287 – 338.
[112] Y. Zheng, A. D. Jensen, P. Glarborg, K. Sendt, B. S. Haynes, *Proc. Combust. Inst.* **2009**, *32*, 1973 – 1980.
[113] P. Dagaut, P. Glarborg, M. U. Alzueta, *Prog. Energy Combust. Sci.* **2008**, *34*, 1 – 46.
[114] F.-J. Tian, J. Yu, L. J. McKenzie, J.-i. Hayashi, C.-Z. Li, *Energy Fuels* **2007**, *21*, 517 – 521.
[115] S. Koger, H. Bockhorn, *Proc. Combust. Inst.* **2005**, *30*, 1201 – 1209.
[116] J. F. Grcar, P. Glarborg, J. B. Bell, M. S. Day, A. Loren, A. D. Jensen, *Proc. Combust. Inst.* **2005**, *30*, 1193 – 1200.
[117] C. Wu, D. Tree, L. Baxter, *Proc. Combust. Inst.* **2007**, *31*, 2787 – 2794.
[118] a) K.-M. Hansson, J. Samuelsson, C. Tullin, L.-E. Åmand, *Combust. Flame* **2004**, *137*, 265 – 277; b) M. Aznar, M. San Anselmo, J. J. Manya, M. B. Murillo, *Energy Fuels* **2009**, *23*, 3236 – 3245.
[119] C. Duinslaegher, H. Jeanmart, J. Vandooren, *Proc. Combust. Inst.* **2009**, *32*, 1277 – 1284.
[120] Z. Tian, Y. Li, L. Zhang, P. Glarborg, F. Qi, *Combust. Flame* **2009**, *156*, 1413 – 1426.
[121] A. Lucassen, P. Oßwald, U. Struckmeier, K. Kohse-Höinghaus, T. Kasper, N. Hansen, T. A. Cool, P. R. Westmoreland, *Proc. Combust. Inst.* **2009**, *32*, 1269 – 1276.
[122] Z. Tian, Y. Li, T. Zhang, A. Zhu, Z. Cui, F. Qi, *Combust. Flame* **2007**, *151*, 347 – 365.
[123] Z. Tian, Y. Li, T. Zhang, A. Zhu, F. Qi, *J. Phys. Chem. A* **2008**, *112*, 13549 – 13555.
[124] S. Yani, D.-k. Zhang, *Proc. Combust. Inst.* **2009**, *32*, 2083 – 2089.
[125] N. W. Tame, B. Z. Dlugogorski, E. M. Kennedy, *Proc. Combust. Inst.* **2009**, *32*, 665 – 671.

